Arteriosclerosis, Thrombosis, and Vascular Biology

BASIC SCIENCES

FSH Is Responsible for Androgen Deprivation Therapy–Associated Atherosclerosis in Mice by Exaggerating Endothelial Inflammation and Monocyte Adhesion

Qiang Wang (王强),* Jingli Han (韩敬丽),* Zhenhui Liang (梁振辉),* Xueyu Geng (耿学妤), Yiqing Du (杜依青), Jing Zhou (周菁), Weijuan Yao (姚伟娟), Tao Xu (徐涛)

BACKGROUND: Androgen deprivation therapy (ADT) is the mainstay treatment for advanced prostate cancer. But ADTs with orchiectomy and gonadotropin-releasing hormone (GnRH) agonist are associated with increased risk of cardiovascular diseases, which appears less significant with GnRH antagonist. The difference of follicle-stimulating hormone (FSH) in ADT modalities is hypothesized to be responsible for ADT-associated cardiovascular diseases.

METHODS: We administered orchiectomy, GnRH agonist, or GnRH antagonist in male *ApoE*$^{-/-}$ mice fed with Western diet and manipulated FSH levels by testosterone and FSH supplementation or FSH antibody to investigate the role of FSH elevation on atherosclerosis. By combining lipidomics, in vitro study, and intraluminal FSHR (FSH receptor) inhibition, we delineated the effects of FSH on endothelium and monocytes and the underlying mechanisms.

RESULTS: Orchiectomy and GnRH agonist, but not GnRH antagonist, induced long- or short-term FSH elevation and significantly accelerated atherogenesis. In orchiectomized and testosterone-supplemented mice, FSH exposure increased atherosclerosis. In GnRH agonist–treated mice, blocking of short FSH surge by anti-FSHβ antibody greatly alleviated endothelial inflammation and delayed atherogenesis. In GnRH antagonist–treated mice, FSH supplementation aggravated atherogenesis. Mechanistically, FSH, synergizing with TNF-α (tumor necrosis factor alpha), exacerbated endothelial inflammation by elevating VCAM-1 (vascular cell adhesion protein 1) expression through the cAMP/PKA (protein kinase A)/CREB (cAMP response element-binding protein)/c-Jun and PI3K (phosphatidylinositol 3 kinase)/AKT (protein kinase B)/GSK-3β (glycogen synthase kinase 3 beta)/GATA-6 (GATA-binding protein 6) pathways. In monocytes, FSH upregulated CD29 (cluster of differentiation 29) expression via the PI3K/AKT/GSK-3β/SP1 (specificity protein 1) pathway and promoted monocyte-endothelial adhesion both in vitro and in vivo. Importantly, FSHR knockdown by shRNA in endothelium of carotid arteries markedly reduced GnRH agonist–induced endothelial inflammation and atherosclerosis in mice.

CONCLUSIONS: FSH is responsible for ADT-associated atherosclerosis by exaggerating endothelial inflammation and promoting monocyte-endothelial adhesion.

GRAPHIC ABSTRACT: A graphic abstract is available for this article.

Key Words: atherosclerosis ■ endothelial cells ■ follicle-stimulating hormone ■ monocytes ■ prostatic neoplasms

Correspondence to: Weijuan Yao, PhD, Department of Physiology and Pathophysiology, Hemorheology Center, School of Basic Medical Sciences, Peking University, No. 38 Xue Yuan Rd, Beijing 100191, China, Email weijuanyao@bjmu.edu.cn; or Tao Xu, MD, Department of Urology, Peking University People's Hospital, No. 11 Xi Zhi Men S St, Beijing 100044, China, Email xutao@pkuph.edu.cn
*Q. Wang, J. Han, and Z. Liang contributed equally.
Supplemental Material is available at https://www.ahajournals.org/doi/suppl/10.1161/ATVBAHA.123.319426.
For Sources of Funding and Disclosures, see page 717.

Arterioscler Thromb Vasc Biol is available at www.ahajournals.org/journal/atvb

Nonstandard Abbreviations and Acronyms

ADT	androgen deprivation therapy
AR	androgen receptor
Bica	bicalutamide
CVD	cardiovascular disease
CYP17A1	cytochrome P450 17A1
Deg	degarelix
eNOS	endothelial NO synthase
FSH	follicle-stimulating hormone
FSHR	follicle-stimulating hormone receptor
GnRH	gonadotropin-releasing hormone
GSK-3β	glycogen synthase kinase 3 beta
HDL	high-density lipoprotein
HUVEC	human umbilical vein endothelial cell
ICAM-1	intercellular adhesion molecule 1
IL	interleukin
LDL	low-density lipoprotein
Leu	leuprolide
LH	luteinizing hormone
MCP-1	monocyte chemoattractant protein 1
NF-κB	nuclear factor kappa B
PCa	prostate cancer
SP1	specificity protein 1
TC	total cholesterol
TG	total triglyceride
TNF-α	tumor necrosis factor alpha
VCAM-1	vascular cell adhesion protein 1

Highlights

- Follicle-stimulating hormone (FSH) is a strong and independent proatherogenic factor.
- The short- and long-term elevation of FSH caused by gonadotropin-releasing hormone agonist and orchiectomy, respectively, results in the aggravation of endothelial inflammation and atherosclerosis development.
- Gonadotropin-releasing hormone antagonist is associated with low cardiovascular disease risk through its effects of lowering the FSH level and altering lipid metabolism.
- FSH synergizing with TNF-α (tumor necrosis factor alpha) stimulates VCAM-1 (vascular cell adhesion protein 1) expression in endothelium through the cAMP/PKA (protein kinase A)/CREB (cAMP response element-binding protein)/c-Jun and the PI3K (phosphatidylinositol 3 kinase)/AKT (protein kinase B)/GSK-3β (glycogen synthase kinase 3 beta)/GATA-6 (GATA-binding protein 6) pathways.
- FSH induces CD29 (cluster of differentiation 29) expression in monocytes via the PI3K/AKT/GSK-3β/SP1 (specificity protein 1) pathway and promotes monocyte adhesion to endothelial cells.

Prostate cancer (PCa) is the second most common malignancy in men worldwide.[1,2] In China, the growth rate of PCa is the first of all cancer species.[3] Androgen deprivation therapy (ADT) has been the standard treatment for advanced and metastatic PCa.[4] Orchiectomy, gonadotropin-releasing hormone (GnRH) agonists, and GnRH antagonists are the 3 types of ADT. ADT significantly decreases the mortality caused by PCa. However, growing clinical trials and observations found that ADT with orchiectomy and GnRH agonists may increase the risk of dying from cardiovascular diseases (CVDs).[5,6] The mortality rate caused by adverse cardiovascular events, such as coronary artery disease, myocardial infarction,[7–9] sudden cardiac death,[10] and stroke,[7,8,11] is as high as 30%, even the same as the specific fatality rate of PCa.[12,13] Therefore, it is urgent and essential to explore the mechanisms for ADT-induced cardiac issues.

Atherosclerosis is a primary vascular disease and prerequisite for almost all adverse cardiovascular events mentioned above. The development and progression of atherosclerosis depends on multiple factors and steps, such as abnormal lipid metabolism,[14] endothelial dysfunction,[15] monocyte adhesion,[16,17] and foam cell formation.[18]

With regard to how ADT induces cardiac complications, it has been speculated that changes in hormone levels with ADT may be an important reason. Several reports have suggested that androgen deficiency can trigger metabolic abnormalities and insulin resistance.[19] Thus, low androgen is considered to be pivotal to ADT-related CVDs. Nevertheless, this could not explain why GnRH antagonist is usually associated with lower risk of CVDs compared with GnRH agonists, although both have comparable castration levels of testosterone.[20,21] Therefore, it is necessary for us to explore other risk factors that may induce adverse cardiovascular events and the potential mechanisms.

Although different types of ADT can make testosterone reach castrated levels, they can also lead to varying degrees of fluctuations in other hormone levels, such as follicle-stimulating hormone (FSH).[22,23] For surgical castration, decreased testosterone level induces continuous elevation of FSH. For GnRH agonist, an initial overstimulation of GnRH receptors leads to a transient surge of FSH. These phenomena do not happen with the GnRH antagonist.[24,25] In addition, studies have found that FSH in GnRH agonist–treated patients does not fall to the level as low as that in GnRH antagonist–treated patients.[25] That is because GnRH agonist primarily suppresses LH (luteinizing hormone), whereas GnRH antagonist suppresses both LH and FSH.[26] The different serum levels of FSH seem to be a prominent distinction among GnRH agonist, GnRH antagonist, and orchiectomy treatments. Researchers started to realize the potential role of FSH in ADT-associated CVDs.[27]

Orchiectomy-induced FSH increase is similar to that in postmenopausal women. In the transitional period of menopause, serum FSH can be maintained at a high concentration for 10 years. Epidemiological evidence suggested that FSH in perimenopausal women was directly related to the number of aortic plaques.[28] It has been reported that higher FSH may increase VCAM-1 (vascular cell adhesion protein 1) expression in endothelial cells, contributing to the development of atherosclerosis in postmenopausal women.[29] It is also shown that human adipocytes express FSHRs (FSH receptors) through which FSH upregulates the genes related to lipid synthesis and results in disorders of lipid metabolism, increasing the risks of atherosclerosis.[23,30] Based on these previous studies, researchers postulated that FSH may at least partially explain the differing effects these ADTs have on CVD risk.[31]

However, more questions remain unanswered: why are both GnRH agonists and surgical castration associated with similar high incidence of CVDs[23] even though they induce different FSH alterations (short versus long term)? Do they share similar mechanisms in inducing CVDs? If the mechanism is related to FSH, what is the molecular basis by which FSH exerts its effects on CVDs? Our recent work showed that exogenous administration of both short- and long-term FSH in *ApoE*$^{-/-}$ mice promoted the formation of plaques characterized with increased macrophage content.[32] Nevertheless, it is still not clear whether the fluctuation of the FSH level is indeed determinant to ADT-associated atherogenesis and what the role of low androgen level is in this context. In addition, although GnRH antagonist is usually considered to be related to lower CVD risk,[23,33,34] the newest randomized controlled study PRONOUNCE (A Trial Comparing Cardiovascular Safety of Degarelix Versus Leuprolide in Patients With Advanced Prostate Cancer and Cardiovascular Disease) showed that GnRH antagonists and agonists did not differ by incidence of cardiovascular end points.[35] Yet, because this trial was stopped prematurely, more studies are still needed to evaluate the association of GnRH antagonist with CVDs. Therefore, to answer these questions and concerns, we performed the present research. By establishing multiple animal models and performing experiments both in vitro and in vivo, we identified the critical role of FSH, elevated either transiently or in the long term, in ADT-associated CVDs by exaggerating endothelial inflammation and promoting monocyte-endothelial adhesion. Moreover, we showed that GnRH antagonist was associated with low CVD risk probably through its roles in lowering the FSH level and altering the lipid metabolism.

MATERIALS AND METHODS

Data Availability

The data, methods, and study materials are available from the corresponding authors to other researchers upon reasonable request. An expanded methods section is available in the Supplemental Methods. The Lipidomics Data Set is available in the Supplemental Material, and all primers are available in Table S1. All research materials are listed in the Major Resources Table in the Supplemental Material.

Mice and Experimental Design

All animal procedures were performed according to the protocols (LA2017095 and LA2021172) approved by the Animal Care and Use Committee of Peking University. Male *ApoE*$^{-/-}$ or C57BL/6J mice purchased from Beijing Vital River Laboratory Animal Technology (Beijing, China) were used for all animal studies. Female mice were excluded in this study because ADT is applied only in males. All results are reported in compliance with the Animal Research: Reporting of In Vivo Experiments guidelines.

For surgical castration model, male *ApoE*$^{-/-}$ mice (7 weeks, 10 mice per group) were anesthetized and sham operated or bilaterally castrated at 7 weeks and allowed to recover for 1 week. Then recombinant FSH (3 IU, Gonal-F; Serono, Sweden) or testosterone (1 mg/kg; MedChemExpress, China) was administrated into mice by subcutaneous injection daily for 12 weeks. All castration mice were fed a Western diet (containing 40% fat and 1.25% cholesterol, No. D12108C; Research Diets) and euthanized at 20 weeks of age. For the GnRH agonist or antagonist administration model, male *ApoE*$^{-/-}$ mice (8 weeks, 10 mice per group) were fed a Western diet for 12 weeks. Leuprolide (Leu; 2 mg/kg; MedChemExpress) or degarelix (Deg; 50 mg/kg; MedChemExpress) was given subcutaneously once a month, respectively. Bicalutamide (Bica; 10 mg/kg; MedChemExpress) was given to Leu-administered mice by gavage once a day. All mice were euthanized at 20 weeks of age. For testosterone or FSH administration model, 4 groups of male *ApoE*$^{-/-}$ mice (8 weeks, 6 mice per group) were fed a Western diet and subjected to daily subcutaneous injection of (1) saline, (2) testosterone (1 mg/kg; MedChemExpress), (3) recombinant FSH (3 IU, Gonal-F; Serono), and (4) testosterone and FSH, respectively, for 8 weeks. Then the mice were euthanized at 16 weeks of age.

For the FSH-blocking experiment, Leu (2 mg/kg) was given subcutaneously to male *ApoE*$^{-/-}$ mice (8 weeks, 8 mice per group) once a month. At the same time, control IgG or anti-FSHβ antibody (200 μg per mouse) was administered per day by intraperitoneal injection for 2 weeks. Anti-FSHβ antibody was a polyclonal antipeptide antibody to a 13-amino-acid-long receptor-binding sequence of the β-subunit of FSH (LVYKDPARPNTQK) generated by GenScript (No. sc1180). Mice were euthanized at 12 or 20 weeks of age for different purposes. For the FSH supplementation experiment, Deg (50 mg/kg; MedChemExpress) was given subcutaneously to male ApoE$^{-/-}$ mice (8 weeks, 6 mice per group) once a month. At the same time, recombinant FSH (3 IU, Gonal-F; Serono) was administrated per day by subcutaneous injection for 2 weeks. Mice were fed a Western diet and euthanized at 20 weeks of age.

For partial carotid artery ligation model, male *ApoE*$^{-/-}$ mice (7 weeks, 8 mice per group) were anesthetized, left common carotid artery closer to the aortic root was clamped with microvessel clamp, and 3 of 4 caudal branches of the left carotid (left external carotid, internal carotid, and occipital artery) were ligated with 5-0 silk suture, while the superior thyroid artery was left intact. Then recombinant adenovirus vector

with FSHR-targeted shRNA (1×10^{11} vp/mL; GenePharma, China) or control virus was injected through the left external carotid and incubated intraluminally for 30 minutes. After the surgery, mice were allowed to recover for 1 week, then Leu (2 mg/kg) was given subcutaneously at 8 weeks. One or 4 weeks after ligation, mice were euthanized for different purposes.

For the observation of monocyte adhesion in vivo, male C57BL/6J mice (8 weeks, 6 mice per group) were anesthetized, and femoral and mesenteric veins were exposed. Human monocytic THP-1 cells with or without FSH treatment were injected into the femoral vein, and monocyte adhesion was observed from mesenteric veins under microscope and recorded for 30 minutes. The number of adherent cells was counted at the 1st, 10th, 20th, and 30th minute, and the average number of these 4 time points was taken as 1 repeat.

Sample Preparation and Histological Analyses

Mice were euthanized and fixed by perfusion through the left cardiac ventricle with 4% paraformaldehyde, then the heart, arterial tree, or ligated carotid arteries were dissected carefully. Left ventricular outflow tracts were fixed in 4% paraformaldehyde and dehydrated in 30% sucrose solution before being frozen in the TissueTek cutting medium (Sakura Finetek). Consecutive 10-μm sections were cut for histological analyses. To quantify atherosclerotic lesions, representative sections where 3 aortic valve leaflets were equally observed were stained with hematoxylin-eosin, oil red O, or Masson trichrome according to the manufacturer's instructions (Solarbio, China). The volume of lesions was calculated by measuring the lesion areas of each section. Area was defined by the internal elastic lamina to the luminal edge of the lesion. Arterial trees were stained with oil red O, and the plaque sizes were quantified by the Image J software (National Institutes of Health). All analyses adhered to the guidelines of AHA Statement for Animal Atherosclerosis Studies.[36]

RESULTS

Long-Term FSH Elevation Is Responsible for Orchiectomy-Accelerated Atherogenesis

To test the role of long-term high FSH level in orchiectomy-associated atherogenesis and distinguish it from loss of protective role of androgen on atherosclerosis, we designed experiments on surgically castrated male *ApoE*$^{-/-}$ mice and manipulated their FSH and testosterone levels. One group of castrated mice was supplemented with testosterone, and another group of castrated mice was administered with both testosterone and FSH (Figure 1A). ELISA data showed that compared with Sham, castration caused low testosterone and high FSH, both of which were recovered by administration of exogenous testosterone; while in testosterone- and FSH-supplemented castrated mice, the FSH level remained as high as in castrated mice even though their testosterone level was similar to Sham mice (Figure 1B and 1C). Oil red O staining showed that atherosclerotic lesions in the aortic root and aortic tree were aggravated in the castrated group compared with Sham but partially alleviated in the castration+testosterone group. Importantly, lesion size in the castration+testosterone+FSH group was aggravated again compared with the castration+testosterone group (Figure 1D and 1E), suggesting a critical role of FSH in plaque formation. Although castration caused body weight loss and the augment of lipid deposit in the liver, testosterone and FSH supplementation did not have much effect on body weight (Figure S1A) or serum/liver/adipose lipids, with one exception that adipose total cholesterol (TC) in castration+testosterone+FSH mice was significantly higher than castration+testosterone mice (Figure S1B through S1I). We measured serum levels of soluble VCAM-1 and MCP-1 (monocyte chemoattractant protein 1), which are the markers for endothelial activation and inflammation. Data showed that both levels were higher in the castrated and castration+testosterone+FSH groups than the Sham and castration+testosterone groups, respectively (Figure 1F and 1G). Collectively, we demonstrated that long-term FSH elevation independent of low androgen level was responsible for orchiectomy-exaggerated inflammation and accelerated atherogenesis.

To further distinguish the roles of testosterone and FSH in atherogenesis, we administered testosterone or FSH in intact male *ApoE*$^{-/-}$ mice for 8 weeks (Figure S2A), which served as a comparison for the experiments performed on castrated mice. ELISA data showed that FSH in the saline and testosterone groups was barely detectable, but FSH levels were high in the FSH and testosterone+FSH groups, respectively (Figure S2B). Surprisingly, testosterone levels in the saline, testosterone, and FSH groups did not show significant difference, although those in the testosterone and FSH groups appeared higher than that in the saline group (Figure S2C). The testosterone level in the testosterone+FSH group was even lower than that in the saline group. Nevertheless, oil red O staining showed that the atherosclerotic lesions in aortic trees and aortic roots were exaggerated in the FSH group as compared with the saline group (Figure S2D through S2G). Testosterone supplement showed some alleviating effects on atherogenesis in the testosterone and testosterone+FSH groups as compared with the saline and FSH groups, respectively. Lipid analyses data showed that serum lipids were rather low in the testosterone, FSH, and testosterone+FSH groups compared with the saline group (Figure S2H through S2K), but there was no difference in the liver or adipose lipids among the groups (Figure S2L through S2O). The data demonstrated the proatherogenic effect of FSH and antiatherogenic effect of testosterone in intact mice, which is consistent with the finding in castrated mice and may not be directly related to their effects on lipid metabolism.

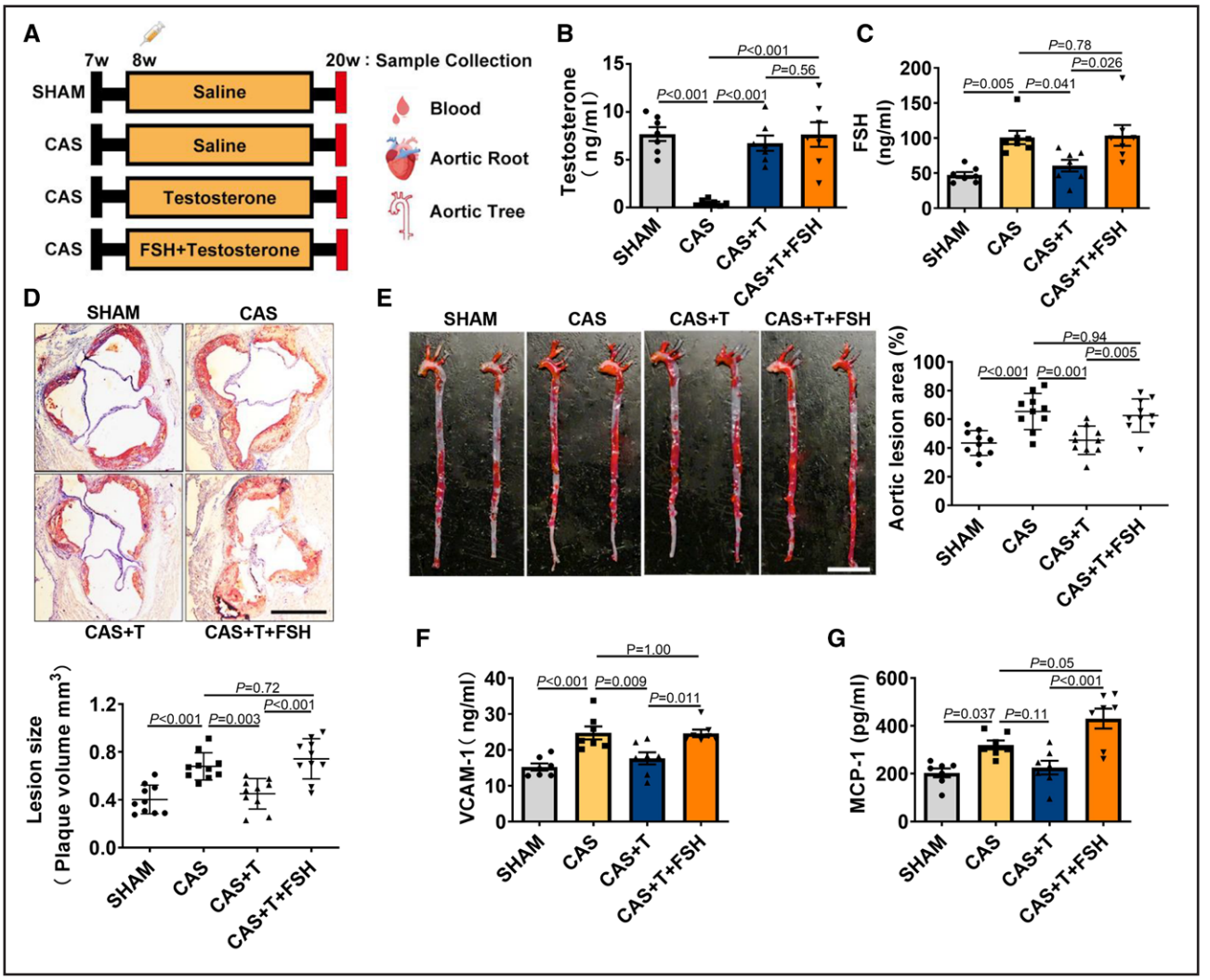

Figure 1. Long-term follicle-stimulating hormone (FSH) elevation is responsible for orchiectomy-accelerated atherogenesis. **A**, The experimental design in which *ApoE*$^{-/-}$ mice were subjected to surgical castration (CAS) at 7 weeks and then subcutaneously injected with FSH, testosterone (T), or both every day from 8 weeks and euthanized at 20 weeks. During this time, mice were fed a Western diet. **B** and **C**, Serum levels of T and FSH in mice of the 4 groups as assessed by ELISA (n=8 mice). **D** and **E**, Oil red O staining of aortic roots (**D**) and aortic trees (**E**) of mice in the sham, CAS, CAS+T, and CAS+T+FSH groups. Representative images of aortic roots are shown in **D** (**top**) and **E** (**left**); scale bar, 500 μm. Two aortic trees are shown for each group (**E**); scale bar, 1 cm. The volumes of plaques in the aortic root and lesion sizes in the aortic tree were quantified and are shown (n=10 mice). **F** and **G**, Serum levels of soluble VCAM-1 (vascular cell adhesion protein 1) and MCP-1 (monocyte chemoattractant protein 1) in mice of the 4 groups as assessed by ELISA (n=8 mice). Data are presented as mean±SEM. Data were analyzed by 1-way ANOVA test followed by the Tukey multiple comparisons test (**B**–**G**).

GnRH Agonist, but Not Antagonist, Induces Increased Atherosclerotic Lesions With Reduced Stabilities

To observe the role of short-term high FSH in GnRH agonist–associated atherosclerosis, we treated high-fat diet–fed male *ApoE*$^{-/-}$ mice with saline, GnRH agonist Leu, GnRH antagonist Deg, and Leu+Bica, respectively (Figure 2A). The reason for adding Bica—a nonsteroidal antiandrogen—was to mimic the drug administration in clinic to reduce adverse effects induced by testosterone surge. In accordance with the clinical observations,[22,23] Deg rapidly reduced FSH and testosterone levels in mice, whereas Leu caused an initial surge of both hormones for 2 weeks followed by gradual decrease (Figure 2B and 2C). Oil red O staining revealed that, as compared with the saline group, the Leu group, as well as the Leu+Bica group, displayed increased atherosclerotic lesions in the aortic root and aortic tree, while the Deg group displayed similar or even smaller lesion sizes (Figure 2D and 2E). Administration of Bica appeared to reduce lesion size in the Leu+Bica group as compared with the Leu group, but this effect was limited and lacked statistical significance. Further analysis of plaque components showed that macrophage content was increased remarkably (Figure 2F), but smooth muscle cell (Figure 2G) and collagen contents (Figure S3A) were significantly decreased in the Leu group, whereas these components

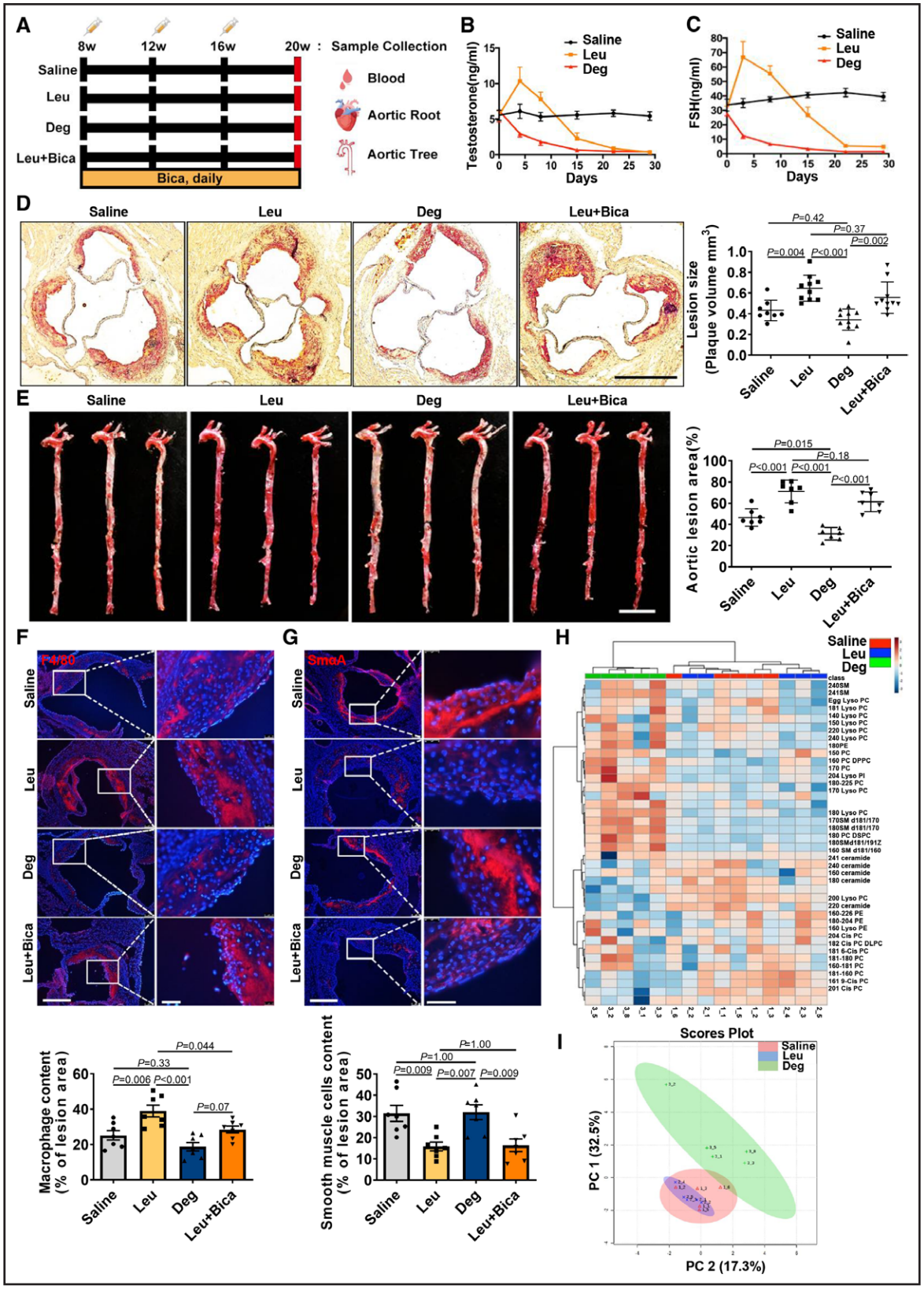

Figure 2. Atherosclerotic lesions increased with reduced stabilities in gonadotropin-releasing hormone (GnRH) agonist–treated mice.

A, The experimental design in which 8-week-old *ApoE*$^{-/-}$ mice were fed a Western diet and subcutaneously injected with saline, leuprolide (Leu), or degarelix (Deg) every month (8, 12, and 16 wk). One group of Leu-injected mice was also fed bicalutamide (Bica). All mice were euthanized at 20 weeks. **B** and **C**, Serum levels of testosterone and follicle-stimulating hormone (FSH) in mice of the 4 groups as (*Continued*)

were barely changed in the Deg group, as compared with control. Bica seemed to lower the macrophage content in plaques. These data indicated that GnRH agonist but not antagonist had a proatherogenic effect and antiandrogens seemed beneficial in a limited range.

Since dyslipidemia is the risk factor for CVDs, we examined whether it was involved in the proatherogenic effect of GnRH agonist. Lipid analysis showed that there were no differences between the Leu and saline groups in their serum TC, total triglyceride (TG), LDL (low-density lipoprotein) cholesterol, HDL (high-density lipoprotein) cholesterol, and body weight, while the Deg group had modest weight loss and higher HDL cholesterol level (Figure S3B through S3F). Surprisingly, the Deg group had much higher liver TC and TG levels than the saline and Leu groups (Figure S3G and S3H). There was no difference in adipose TC and TG among the 3 groups (Figure S3I and S3J). We further analyzed phospholipid compositions in the serum by lipidomics and discovered that no obvious differences were seen between the saline and Leu groups, whereas the Deg group exhibited a distinct phospholipid profile (Figure 2H; Lipidomics Data Set in the Supplemental Material). Deg caused the increase of lysophosphatidylcholines and the reduction of ceramides. Besides, principal component analysis discriminated the Deg group from the others (Figure 2I). These findings indicate that GnRH agonist and antagonist have distinct effects on atherosclerosis possibly through different mechanisms. The surges of testosterone and FSH was the major difference between Leu and Deg administration. Based on our data, it is reasonable to hypothesize that shortly elevated FSH may play an imperative role in GnRH agonist–associated atherosclerosis.

Short-Term FSH Elevation Is Critical to GnRH Agonist–Associated Atherogenesis

To prove that the enhanced atherosclerosis in Leu-administered mice indeed resulted from the short-term FSH elevation, we tried to block FSH activity by injecting specific anti-FSHβ antibody[37,38] to Leu-administered mice during the first 2 weeks, when the FSH surge occurs (Figure 3A). Analyses of atherosclerotic lesions at week 20 showed that anti-FSHβ antibody treatment led to strikingly reduced lesion size in both the aortic root and aortic tree (Figure 3B and 3C). Since anti-FSHβ antibody had no effects on body weight (Figure S4A) and proportions of monocytes in blood and bone marrow (Figure S4B through S4E), we believed that its beneficial effect was derived from antagonizing FSH activity. Furthermore, we added FSH in the first 2 weeks to Deg-administered *ApoE*$^{-/-}$ mice, imitating the FSH surge that occurs in Leu-administered mice (Figure 3D and 3E). Analyses performed at week 20 showed that, in consistency with the results of Leu treatment, atherosclerotic lesions in the Deg+FSH group remarkably expanded in both the aortic root and aortic tree as compared with the Deg group (Figure 3F and 3G). Taken together, these data indicated that, like long-term elevation of FSH, short-term elevation of FSH also exaggerated atherosclerosis progression, and importantly, it was critical to GnRH agonist–associated atherogenesis.

FSH Synergizing With TNF-α Exacerbates Endothelial Inflammation

Next, we sought to investigate the pathological role of FSH on atherosclerosis. We noticed that macrophage content significantly increased in Leu-exposed mice. The major source of plaque macrophages is circulating monocytes in the blood, which adhere to vascular endothelium and then migrate across the endothelium and differentiate into macrophages underneath intima.[16,39] Endothelial inflammation and dysfunction promote monocyte adhesion and migration.[15,40] The increased serum VCAM-1 and MCP-1 levels in castrated and castration+testosterone+FSH mice indicated that high FSH should be related to endothelial inflammation. Therefore, we tried to explore the proatherogenic effect of FSH on endothelium in vitro. We first confirmed FSHR expression on human umbilical vein endothelial cells (HUVECs; Figure S5B) as reported previously.[41] Then we treated HUVECs with FSH to further investigate the functional role of FSH/FSHR. It is reported that the testosterone level in culture medium containing 10% FBS (fetal bovine serum) was ≈0.03 nmol/L, which has marginal effect on AR (androgen receptor).[42] Therefore, we considered the culture medium as androgen low or depleted medium, which mimicked

Figure 2 Continued. assessed by ELISA (n=8 mice). **D**, Oil red O staining of aortic roots of mice in the saline, Leu, Deg, and Leu+Bica groups. Representative images are shown with a 500-μm scale bar. The volumes of plaques were quantified (n=8–10 mice). **E**, Oil red O staining of aortic trees of mice in the 4 groups. Three aortic trees were shown for each group. Scale bar, 1 cm. The lesion sizes were quantified (n=7 mice). **F**, SmαA (smooth muscle α-actin) immunostaining (red) on the plaques of aortic roots of mice. Representative images are shown in the **left** (scale bar, 300 μm) and higher magnification images for boxed areas are on the **right** (scale bar, 50 μm). The SMαA$^+$ areas were measured to indicate smooth muscle cell content (n=7 mice). **G**, F4/80 immunostaining (red) on the plaques of aortic roots of mice. Representative images are shown in the **left** (scale bar, 300 μm) and higher magnification images for boxed areas are on the **right** (scale bar, 50 μm). The F4/80$^+$ areas were measured to indicate macrophage content (n=7 mice). **H**, Heat map of significantly altered serum lipids of mice in the saline, Leu, and Deg groups. The color of each section is proportional to the significance of the change in metabolites (red, upregulated; blue, downregulated; n=5 mice). **I**, Principal component (PC) analysis score plots based on phospholipid profiles of the saline, Leu, and Deg groups (n=5 mice). Data are presented as mean±SEM. Data were analyzed by 1-way ANOVA test followed by the Tukey multiple comparisons test (**D**–**G**).

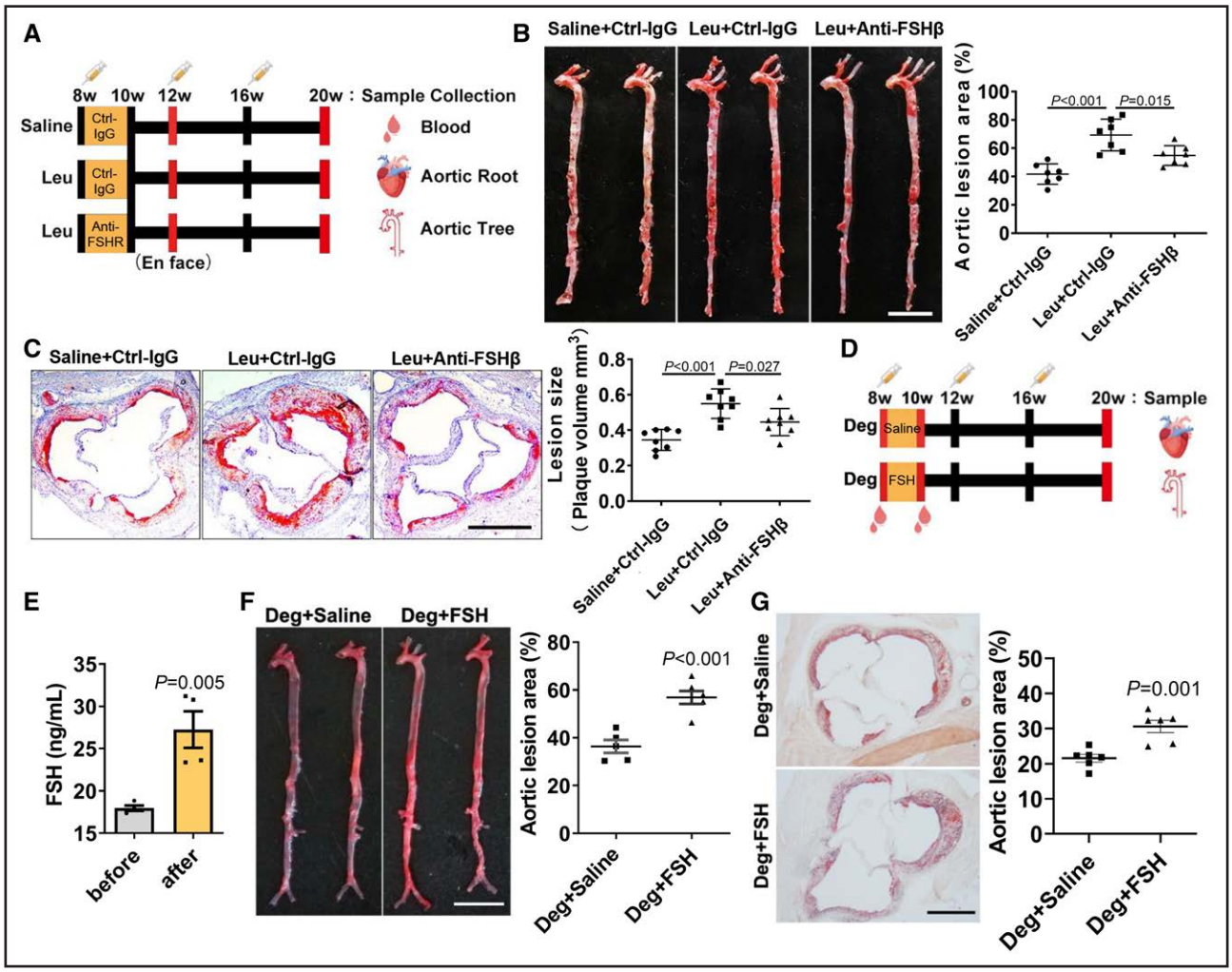

Figure 3. Short-term follicle-stimulating hormone (FSH) elevation is critical to gonadotropin-releasing hormone (GnRH) agonist–associated atherogenesis.

A, The experimental design in which 8-week-old *ApoE*$^{-/-}$ mice were subcutaneously injected with leuprolide (Leu) every month (8, 12, and 16 wk) and supplemented with the anti-FSHβ antibody or control IgG intraperitoneally during the first 2 weeks (8–10 wk). Mice were fed a Western diet and euthanized at 12 or 20 weeks. **B** and **C**, Oil red O staining of aortic trees (**B**) and aortic roots (**C**) of mice in the saline, Leu+Ctrl-IgG, and Leu+anti-FSHβ groups. Representative images of aortic roots are shown in the **left** (**B**). Scale bar, 500 μm. Two aortic trees were shown for each group (**C**). Scale bar, 1 cm. The volumes of plaques in the aortic root and the lesion sizes in the aortic tree were quantified and are shown (n=7–8 mice). **D**, The experimental design in which 8-week-old *ApoE*$^{-/-}$ mice were subcutaneously injected with degarelix (Deg) every month (8, 12, and 16 wk) and supplemented with FSH or saline intraperitoneally during the first 2 weeks (8–10 wk). Mice were fed a Western diet and euthanized at 20 weeks. **E**, Serum levels of FSH in mice of the Deg+FSH group as assessed by ELISA before and after FSH supplementation (n=4 mice). **F** and **G**, Oil red O staining of aortic trees (**F**) and aortic roots (**G**) of mice in the Deg+saline and Deg+FSH groups. Representative images are shown in the **left**. Scale bars, 1 cm (**F**) and 500 μm (**G**). The lesion sizes in the aortic tree and the plaques in the aortic root were quantified and are shown in the **right** (n=6 mice). Data are presented as mean±SEM. Data were analyzed by 1-way ANOVA test followed by the Tukey multiple comparisons test (**B** and **C**) and by the unpaired, 2-tailed Student *t* test (**E**–**G**). Ctrl indicates control.

the in vivo condition. Interestingly, FSH alone exerted no proinflammatory effects on HUVECs, but in synergy with TNF-α (tumor necrosis factor alpha), a proinflammatory factor, FSH remarkably augmented the expression of VCAM-1, E-selectin, and MCP-1 (Figure 4A through 4F). We found that FSH, once coupled with TNF-α, promoted HUVECs to secrete higher levels of MCP-1 and increased numbers of THP-1 adhesion with HUVECs than TNF-α alone (Figure 4G through 4I). We also identified that 50 ng/mL was the optimal concentration of FSH that had the maximum synergistic effect with TNF-α on endothelial inflammation (Figure S5C), a concentration that is close to GnRH agonist–related FSH surge. Unlike FSH, LH or GnRH agonist Leu itself had no effect on HUVECs, who express LH or GnRH receptors (data not shown), in terms of inflammatory gene expression, excluding these potential confounding factors on endothelial inflammation (Figure S5A through S5D). Additionally, we found that FSH did not affect the proliferation and migration of HUVECs (Figure S5E and S5F), excluding

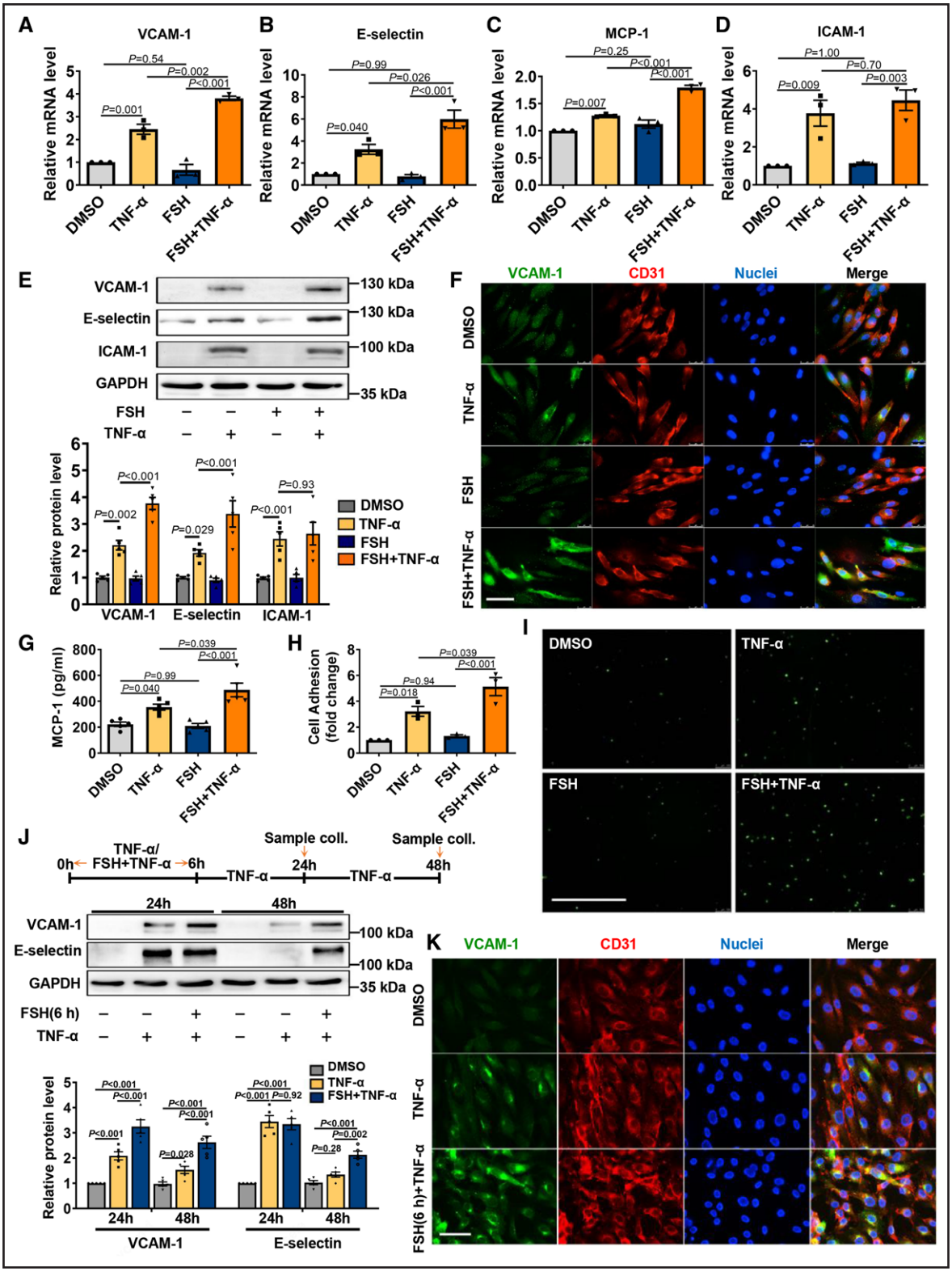

Figure 4. Follicle-stimulating hormone (FSH) synergized with TNF-α (tumor necrosis factor alpha) to enhance the expression of adhesion molecules in the endothelium.

Human umbilical vein endothelial cells (HUVECs) were treated with dimethyl sulfoxide (DMSO), TNF-α (10 ng/mL), FSH (50 ng/mL), or FSH and TNF-α for 24 hours (**A**–**I**); or TNF-α (10 ng/mL) for 24 or 48 hours, the combination of FSH and TNF-α for 6 hours following only TNF-α for 24 or 48 hours (**J** and **K**). **A** through **E**, The effects of DMSO, TNF-α, FSH, or FSH and TNF-α on the expression of adhesion molecules were determined by qRT-PCR (quantitative reverse transcription-polymerase chain reaction; **A**–**D**, n=3 biological replicates) and Western blotting (**E**, n=4 biological replicates). GAPDH was used as a loading control. **F**, Representative images of VCAM-1 (vascular cell adhesion protein 1; green) in HUVECs (CD31 [cluster of differentiation 31] positive, red) with the indicated treatment were determined (*Continued*)

other possible effects of FSH on endothelial cells. Importantly, the expression of VCAM-1, E-selectin, and MCP-1 was also found increased significantly on aortic endothelium in castrated and castration+testosterone+FSH mice compared with Sham and castration+testosterone mice, respectively (Figure S6A through S6D), confirming that FSH indeed exaggerated endothelial inflammation in vivo.

To find out whether transient elevation of FSH, which occurs in Leu administration, also has a proatherogenic effect on endothelial cells, we mimicked this process in vitro: with continued stimulation by TNF-α (24 and 48 hours), FSH was used to transiently treat HUVECs in the first 6 hours and then removed. We found that, without FSH, expressions of VCAM-1 and E-selectin were upregulated at 24 hours but totally faded at 48 hours, whereas with transient treatment of FSH, VCAM-1 expression became even stronger at 24 hours and most importantly, VCAM-1 and E-selectin expressions remained at high level till 48 hours (Figure 4J), which was clearly demonstrated by immunostaining (Figure 4K). This phenomenon was also true in vivo because our immunostaining showed that there were much stronger VCAM-1 and E-selectin signals on the atherosclerotic plaques of Leu-administered mice than saline- or Deg-administered mice (Figure S5G and S5H). Moreover, en face staining of aorta collected 4 weeks after Leu or Leu+anti-FSHβ administration revealed that anti-FSHβ antibody remarkably inhibited VCAM-1 expression in the endothelium (Figure S6E), indicating that inhibition of FSH activity alleviated endothelial inflammation in the early stages of atherosclerosis induced by Leu. Collectively, these data suggest that FSH increased the sensitivity of endothelial cells to cytokines and that, in synergy with TNF-α, it exacerbated endothelial inflammation and dysfunction.

Considering multiple proinflammatory factors exist in the blood of patients with preexisting CVDs, we next determined whether FSH could synergize with other proinflammatory factors, such as IL (interleukin)-1β. HUVECs were treated with IL-1β and FSH, and the expression of adhesion molecules was detected. Data showed that FSH, in synergy with IL-1β, augmented the expression of VCAM-1, E-selectin, ICAM-1 (intercellular adhesion molecule 1), and MCP-1 (Figure S7A through S7D) and significantly increased the protein expression of VCAM-1 (Figure S7E and S7F). In addition, previous study showed that androgen exposure increased human monocyte adhesion to ECs and EC expression of VCAM-1.[43] To exclude the possibility that testosterone surge occurred in Leu administration or testosterone supplement in castrated mice might exert adverse effect on endothelial cells, we treated HUVECs with testosterone and TNF-α and examined the expression of adhesion molecules. Results showed that neither testosterone alone nor testosterone+TNF-α could increase the expression of VCAM-1, E-selectin, and ICAM-1 (Figure S7G through S7K). In addition, to demonstrate whether the synergistic effect of FSH and proinflammatory factors would also be observed with arterial endothelial cells, additional experiments were performed with human aortic endothelial cells. Similar to HUVECs, human aortic endothelial cells treated with FSH+IL-1β showed significantly enhanced expression of VCAM-1 (Figure S7L through S7Q).

FSH Promotes Adhesion of Monocytes to Endothelial Cells

In addition to endothelial cells, the circulating monocytes would be subjected to high level of FSH upon GnRH agonist or orchiectomy administration. We then explored whether FSH could modulate adhesion of monocytes to resting HUVEC monolayer. Data showed that monocyte-endothelial adhesion was remarkably enhanced in the FSH treatment group compared with the control group (Figure 5A and 5B), which was reversed by FSHR blockade (Figure 5C and 5D). Exposure of FSH to human CD (cluser of differentiation) $14^{+}CD11b^{+}$ monocytes isolated from human peripheral blood mononuclear cells also increased their adhesion to HUVECs (P=0.0025; Figure 5E; Figure S8D). Furthermore, we injected FSH-treated THP-1 cells into femoral veins of wild-type mice and observed the in vivo monocyte adhesion from the mesenteric veins under microscope. Data showed that FSH triggered firm adhesion (adhesion time was ≥10 s) of monocytes to vascular wall (Figure 5F; Videos S1 through S3) even though the rolling adhesion was not changed too much.

Next, we explored whether FSH-modulated factors closely related to adhesion, such as CD29, L-selectin, ITGAL (integrin subunit alpha L), ICAM-1, and C-X-C motif chemokine 1. Results showed that CD29 and L-selectin were significantly elevated after FSH exposure (Figure 5G and 5H; Figure S8A). Both immunofluorescence and flow cytometry analysis clearly demonstrated the enriched expression of CD29 (Figure 5I and 5J) and L-selectin (Figure S8B) on FSH-treated THP-1 cell

Figure 4 Continued. using immunofluorescence (IF). Scale bar, 50 μm. **G**, Levels of MCP-1 (monocyte chemoattractant protein 1) in culture media of HUVECs with the indicated treatment as assessed by ELISA; n=5 biological replicates. **H** and **I**, The adhesion of GFP (green fluorescent protein)-labeled human monocytic THP-1 cells to HUVECs with the indicated treatment was observed under a fluorescence microscope (scale bar, 300 μm). The adhered cell numbers were counted from images of 3 biological replicates, and the data are shown as the fold change (ratio to DMSO). **J**, Effect of transient stimulation with FSH (6 h) on VCAM-1 and E-selectin expression by Western blotting. n=4 biological replicates. **K**, Representative images of VCAM-1 (green) in HUVECs (CD31 positive, red) with the indicated treatment (24 h) were determined using IF. Scale bar, 50 μm. Data are presented as mean±SEM. Data were analyzed by 1-way ANOVA test followed by the Tukey multiple comparisons test (**A**–**D**, **G**, and **H**) and by 2-way ANOVA test followed by the Tukey multiple comparisons test (**E** and **J**). Sample coll. indicates sample collection.

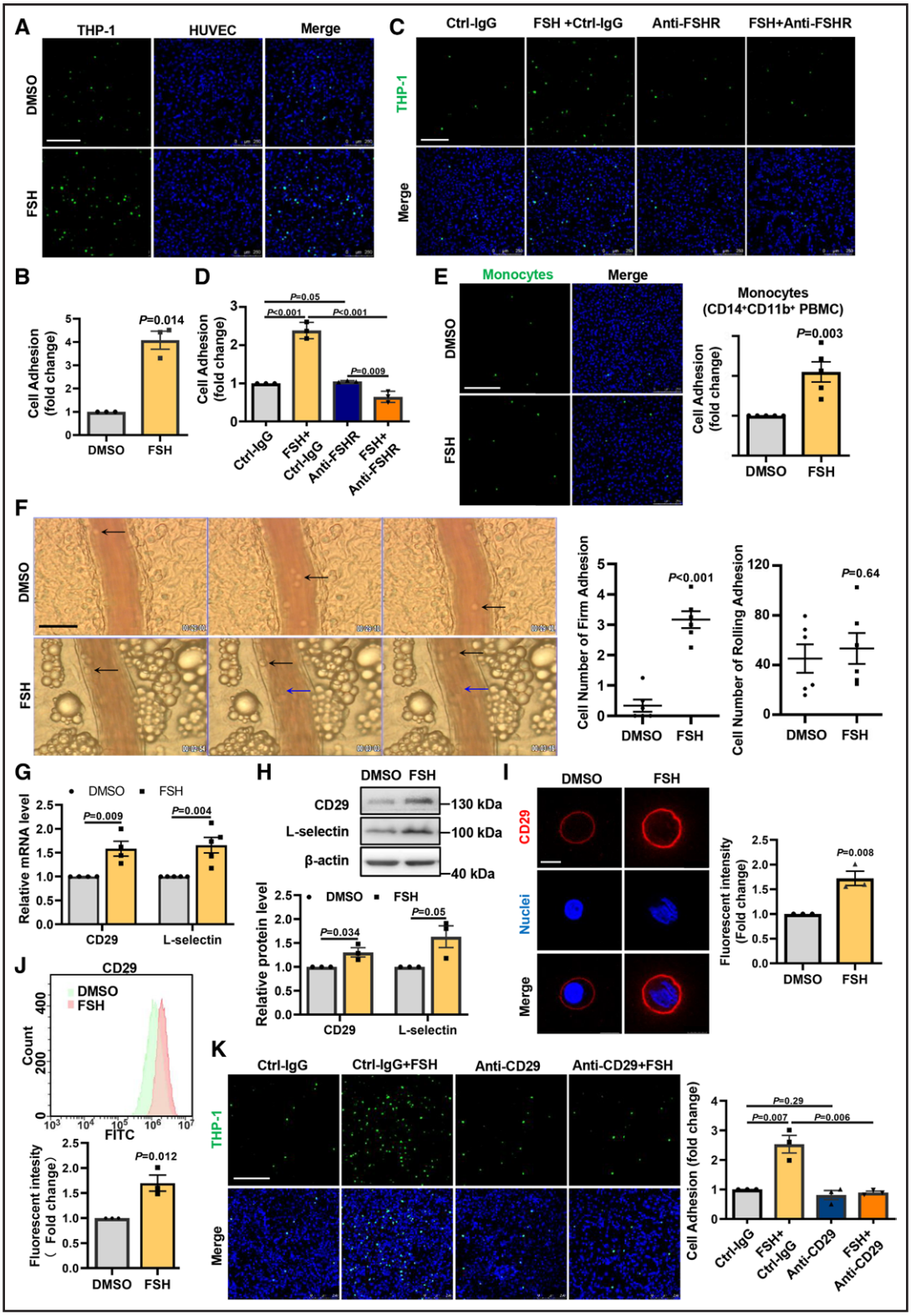

Figure 5. Follicle-stimulating hormone (FSH) promoted adhesion of monocytes to endothelium.
Human monocytic THP-1 cells and human primary CD11b$^+$CD14$^+$ cells were infected with GFP (green fluorescent protein) adenovirus for 48 hours, treated with FSH (50 ng/mL) for 24 hours, and then cocultured with human umbilical vein endothelial cells (HUVECs; **A**–**E**, and **K**). THP-1 cells were exposed to FSH (50 ng/mL) for 24 hours (**F**–**J**). **A** and **B**, The effect of FSH on the adhesion of THP-1 cells to resting HUVEC monolayers (scale bar, 300 μm); n=3 biological replicates. **C** and **D**, The effects of FSH, anti-FSHR (FSH receptor) antibody on THP-1 cell adhesion. GFP-labeled THP-1 cells with anti-FSHR antibody or control (Ctrl) IgG pretreatment were treated with FSH and then cocultured with HUVECs. Scale bar, 300 μm; n=6 mice. **E**, The effect of FSH on the adhesion of CD11b$^+$CD14$^+$ monocytes (n=5 biological replicates; scale bar, 300 μm). **F**, The effect of FSH on the adhesion of THP-1 cells in the normal blood flow of wild-type C57BL/6 mice. (*Continued*)

membrane. Time course study showed that the effect of FSH on CD29 and L-selectin expression could last for 72 and 48 hours, respectively (Figure S8C). Moreover, we also observed the upregulation of CD29 in peripheral blood mononuclear cells of FSH-treated mice (Figure S8E and S8F). Most importantly, when CD29 was specifically blocked by CD29-blocking antibody, the effect of FSH on monocyte adhesion was eliminated (Figure 5K). Therefore, CD29 may play a leading role in FSH-promoted monocyte adhesion. Meanwhile, we excluded the possibility of ADT drugs, Leu and Deg, in regulating monocyte adhesion (Figure S8G and S8H). We detected the monocyte migration by transwell assay but did not find any effect of FSH (Figure S8I). Our data suggest that, in addition to exaggerating endothelial inflammation, FSH could also promote monocyte adhesion to endothelial cells by upregulating CD29. These 2 effects of FSH make FSH become a strong proatherogenic factor. We also examined the effects of FSH on macrophages and found that FSH promoted macrophage migration to MCP-1 and decreased its spreading ability (Figure S9A through S9E). These suggest that FSH had a proinflammatory effect on macrophages.

FSHR/cAMP/PKA/CREB/c-Jun and PI3K/AKT/GSK-3β/GATA-6 Pathways Are Involved in Synergistic Action of FSH and TNF-α on Endothelial Inflammation

Next, we sought to explore the molecular mechanisms for the synergistic effect of FSH and TNF-α on endothelial inflammation. cAMP/PKA (protein kinase A)/CREB (cAMP response element-binding protein), PI3K (phosphatidylinositol 3 kinase)/AKT (protein kinase B), p38 MAPK (mitogen-activated protein kinase), and MEK (mitogen-activated protein kinase/ERK (extracellular signal regulated kinase) are the major pathways downstream of FSHR.[41,44,45] We found that FSH+TNF-α dramatically increased phosphorylation of CREB and AKT compared with FSH or TNF-α alone (Figure 6A through 6C). Then we blocked FSHR and the downstream pathways by antibody or inhibitors to find out which pathway is responsible for FSH+TNF-α–amplified endothelial inflammation. Results showed that anti-FSHR antibody, PKA inhibitor (H89), and PI3K inhibitor (LY294002) all eliminated FSH+TNF-α–induced upregulations of VCAM-1 and E-selectin (Figure 6A through 6C) except the MEK inhibitor (PD98059; Figure S10A). Although the p38 MAPK inhibitor (SB203580) partially inhibited VCAM-1 expression, it had a converse effect on E-selectin (Figure S10B), suggesting the different regulations of the p38 MAPK pathway on these 2 adhesion molecules. Of note, the NF-κB (nuclear factor kappa B) pathway was not involved in FSH+TNF-α–induced VCAM-1 expression since there were little changes in its activated NF-κB level as compared with TNF-α alone (Figure S10F).

CREB can bind CRE (cAMP responsive element)/AP-1 (activator protein 1) box together with c-Jun and regulates transcriptions of several genes, including *VCAM-1*.[46,47] Similar to CREB phosphorylation, c-Jun phosphorylation was augmented by FSH+TNF-α (Figure 6D and 6E), and both phosphorylated CREB and c-Jun could be suppressed by the PKA inhibitor or PKAα siRNA (Figure 6B and 6D; Figure S10C). Besides, GSK-3β (glycogen synthase kinase 3 beta)—a target of the PI3K/AKT pathway—was shown critical for TNF-α–induced VCAM-1 expression in endothelial cells.[40,48] We detected increased GSK-3β phosphorylation in FSH+TNF-α–treated HUVECs, which could be blocked by specific inhibition of the PI3K/AKT pathway (Figure 6E; Figure S10D). But neither c-Jun nor CREB phosphorylation could be reversed by p85α siRNA (Figure 6E). These data suggested that the FSHR/cAMP/PKA/CREB and the PI3K/AKT/GSK-3β pathways were involved in FSH+TNF-α–induced upregulation of VCAM-1 and E-selectin.

Since CREB and c-Jun occupied common binding sites and were similarly regulated by FSH+TNF-α, we were interested to see whether they could interact with each other. Unfortunately, coimmunoprecipitation assay failed to detect their binding potential (Figure S10G). Then we suppressed CREB expression with a plasmid encoding dominant-negative CREB (known as A-CREB)[49] and found that FSH+TNF-α–induced upregulations of VCAM-1 and E-selectin were markedly reversed. Similar changes were seen in c-Jun expression (Figure S10E), suggesting that c-Jun acts downstream of CREB. Furthermore, c-Jun knockdown effectively suppressed FSH+TNF-α–induced VCAM-1 and E-selectin expressions (Figure 6F). The chromatin immunoprecipitation assay indeed confirmed that enrichment of c-Jun on the VCAM-1 promoter was significantly increased by FSH+TNF-α treatment (Figure 6G).

Figure 5 Continued. Representative statistics about the number of firm adhesion and rolling adhesion THP-1 cells are shown on the **right**. Black arrows indicate rolling adhesion THP-1 cells, and blue arrows indicate firm adhesion THP-1 cells (n=6 mice; scale bar, 50 μm). **G** and **H**, The effects of FSH on the expression of adherent molecules were determined by qRT-PCR (quantitative reverse transcription polymerase chain reaction; **G**, n=5 biological replicates) and Western blotting (**H**, n=3 biological replicates). **I** and **J**, The effects of FSH on membrane CD29 were determined by immunofluorescence (**I**) and flow cytometry (**J**); n=3 biological replicates. **K**, The effect of anti-CD29 antibody on the adhesion of THP-1 cells. THP-1 cells with the indicated FSH treatment were exposed to anti-CD29 antibody or Ctrl-IgG antibody for 1 hour and then cocultured with HUVECs (scale bar, 300 μm); n=3 biological replicates. Data are presented as mean±SEM. Data were analyzed by unpaired, 2-tailed Student *t* test (**B** and **E–J**) and by 1-way ANOVA test followed by the Tukey multiple comparisons test (**K**). CD indicates cluster of differentiation; DMSO, dimethyl sulfoxide; FITC, fluorescein isothiocyanate; and PBMC, peripheral blood mononuclear cell.

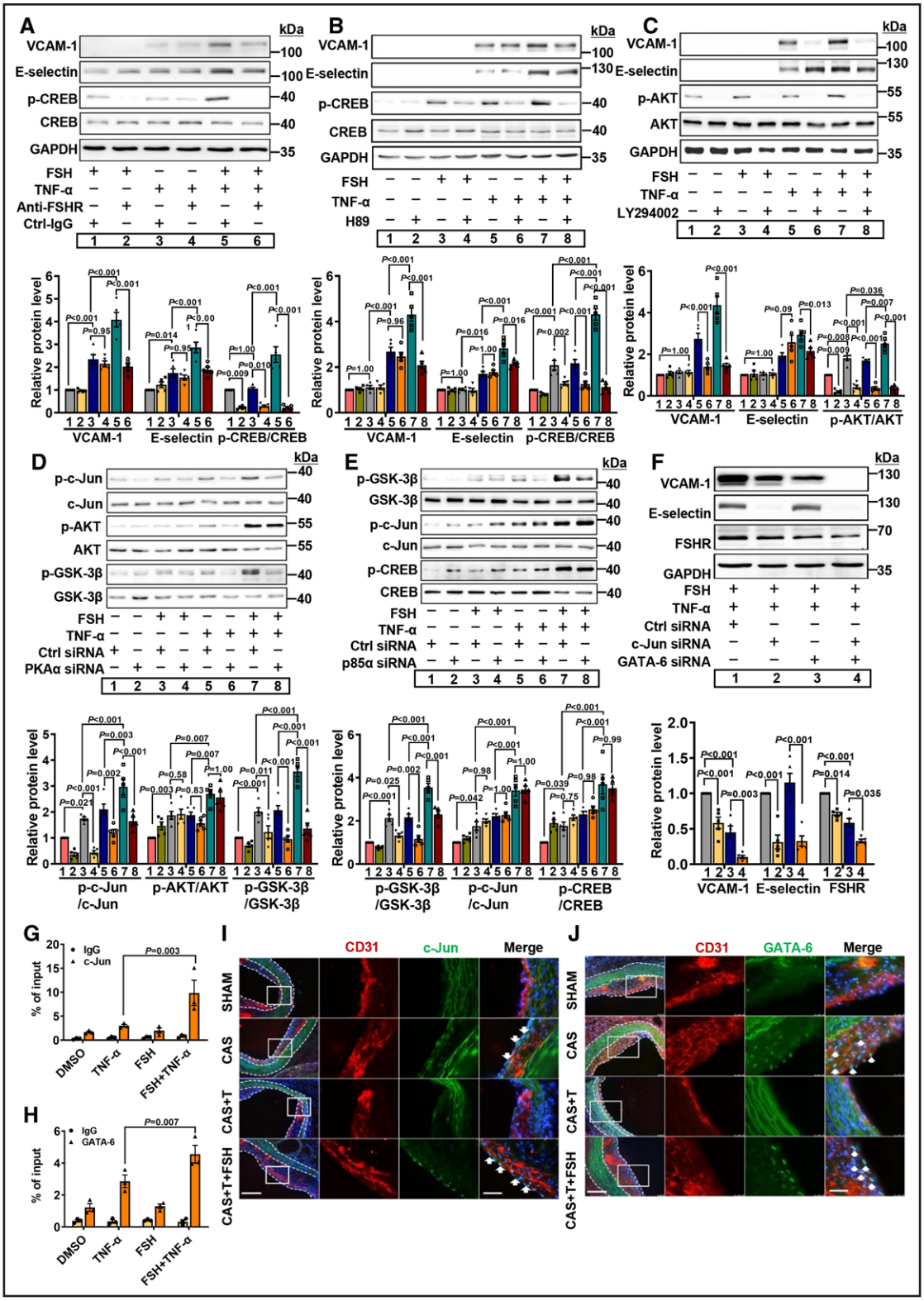

Figure 6. The cAMP/PKA (protein kinase A)/CREB (cAMP response element-binding protein) and the PI3K (phosphatidylinositol 3 kinase)/AKT (protein kinase B)/GSK-3β (glycogen synthase kinase 3 beta) pathways were involved in the synergistic action of follicle-stimulating hormone (FSH) and TNF-α (tumor necrosis factor alpha) on endothelial inflammation, tightly regarding the transcription factors c-Jun and GATA-6 (GATA-binding protein 6).

Human umbilical vein endothelial cells (HUVECs) were pretreated with the FSHR (FSH receptor) antibody, PKA inhibitor H89 (10 μM), PI3K inhibitor LY294002 (10 μM), or FSHR antibody for 1 hour and then treated with TNF-α (10 ng/mL), FSH (50 ng/mL), or FSH+TNF-α for 6 hours. **A**, The effects of FSHR blockade on the expression of VCAM-1 (vascular cell adhesion protein 1), E-selectin, phosphorylated CREB (p-CREB), and total CREB in HUVECs with the indicated treatment. GAPDH served as a loading control (Ctrl); n=5 biological replicates. (*Continued*)

In HUVECs, GATA-6 (GATA-binding protein 6) exclusively binds to GSK-3β, preventing its binding with the VCAM-1 promoter, while GSK-3β phosphorylation leads to the disruption of the GSK-3β/GATA-6 complex.[50] Since FSH+TNF-α induced extensive GSK-3β phosphorylation, increased GATA-6 binding with VCAM-1 promoter would be expected. Chromatin immunoprecipitation assays confirmed that FSH+TNF-α treatment caused enhanced binding of GATA-6 on the *VCAM-1* promoter (Figure 6H). Similarly, GATA-6 knockdown effectively suppressed FSH+TNF-α–induced VCAM-1 expression but not E-selectin expression (Figure 6F). We further knocked down c-Jun and GATA-6 simultaneously and found that FSH+TNF-α–induced VCAM-1 expression was totally eliminated (Figure 6F). Consistently, increased expressions of c-Jun and GATA-6 were indeed detected in plaques of castrated *ApoE*$^{-/-}$ mice with or without testosterone+FSH supplement (Figure 6I and 6J). The results above supported that FSH, synergizing with TNF-α, activates c-Jun and GATA-6 mainly through the cAMP/PKA/CREB and the PI3K/AKT/GSK-3β pathways, thus promoting VCAM-1 expression and endothelial inflammation.

FSH Upregulates CD29 Through the PI3K/AKT/GSK-3β/SP1 Signaling Pathway in Monocytes

We further checked whether the signaling pathways mentioned above were involved in CD29 expression in monocytes. Results showed that blocking FSHR with antibody greatly suppressed FSH-induced CD29 upregulation (Figure 7A). FSH activated AKT via phosphorylation and induced GSK-3β phosphorylation (Figure 7B and 7E; Figure S11A). Importantly, inhibition of the PI3K/AKT pathway by the PI3K inhibitor LY294002 and p85α siRNA inverted FSH-induced CD29 upregulation (Figure 7B; Figure S11A). The PI3K inhibitor also eliminated the effects of FSH on monocyte-HUVEC adhesion and the level of membrane CD29 (Figure 7C and 7D). In addition, FSH did not induce the activation of CREB, ERK, and p38, and unsurprisingly, inhibition of PKA, ERK, and p38 by H89, PD98059, and SB253580 had no effect on CD29 upregulation induced by FSH (Figure S11B through S11D). Therefore, FSH regulated CD29 expression predominantly through the PI3K/AKT/GSK-3β signaling pathway in monocytes.

We performed transcription factor analysis on the TFsitescan website and found that multiple transcription factors could potentially bind to the CD29 promoter, among which SP1 (specificity protein 1) and NF-κB had higher scores. NF-κB is a classic transcriptional factor downstream the PI3K/AKT pathway. SP1 could bind to the GC box (GGGCGG) to affect transcription and would degrade after phosphorylation.[51] Therefore, NF-κB, SP1, and their phosphorylation levels were measured in FSH-treated monocytes. Results showed that SP1 was upregulated and phosphorylated SP1 was decreased by FSH exposure, which could be eliminated by the PI3K inhibitor (Figure 7E). NF-κB and phosphorylated NF-κB were not changed by FSH (Figure S11E). When we knocked down SP1 expression by siRNA (Figure S11F), CD29 expression was remarkably attenuated in FSH-treated THP-1 cells (Figure 7F). These results indicated that SP1 played a crucial role in FSH-induced upregulation of CD29.

The enhanced SP1 expression induced by FSH may be due to the inhibition of SP1 phosphorylation as shown in Figure 7E. Less SP1 phosphorylation prevented its degradation. By transfecting THP-1 cells with an SP1 luciferase reporter, we found that SP1 transcriptional activity was significantly increased by FSH (Figure 7G), suggesting that the transcriptional regulation of SP1 by FSH exists. Furthermore, it was reported that GSK-3β could interact with SP1 and phosphorylation of GSK-3β could destroy their interaction, making free SP1 enter the nucleus to further bind to the promoter of the regulated genes.[51] Coimmunoprecipitation assay showed that the interaction of GSK-3β and SP1 was immensely reduced by FSH (Figure 7H). Moreover, the FSH-reinforced binding of SP1 on the *CD29* promoter was verified by chromatin immunoprecipitation assays (Figure 7I). Consistent with the above data, immunofluorescence revealed the strikingly accumulated SP1 signals in nuclei of FSH-treated THP-1 cells, which was inverted by PI3K inhibition (Figure 7J). These results indicated that FSH promoted phosphorylation of GSK-3β through PI3K/AKT and reduced the binding of GSK-3β and SP1, which allowed the freed SP1 to enter the nucleus to bind with the *CD29* promoter and promote its gene expression.

Figure 6 Continued. **B** and **C**, The effects of PKA inhibitor H89 (**B**) and PI3K inhibitor LY204002 (**C**) on the expression of VCAM-1 and E-selectin in HUVECs. p-CREB, total CREB, phosphorylated AKT (p-AKT), and total AKT were also detected to indicate the effectiveness of inhibitors; n=5 biological replicates. **D** and **E**, The effects of PKAα knockdown (**D**) and p85α knockdown (**E**) on the Gαs (G-protein alpha s)/cAMP/PKA/CREB and the PI3K/AKT/GSK-3β pathways in HUVECs; n=5 biological replicates. **F**, The effect of simultaneous c-Jun and GATA-6 knockdown on VCAM-1 and FSHR expression in HUVECs; n=5 biological replicates. **G** and **H**, Enrichment of c-Jun and GATA-6 on VCAM-1 promoter as determined by the chromatin immunoprecipitation assay in HUVECs with indicated treatment for 6 hours. IgG was served as negative Ctrl; n=3 biological replicates. **I** and **J**, Representative images of c-Jun (**I**, green) and GATA-6 (**J**, green) in the endothelium (CD31 positive, red) of the ascending aorta of mice (n=8) were determined using immunofluorescence (IF). Scale bar, 50 μm. Higher magnification images for boxed areas are shown in the **right**. Scale bar, 25 μm. White arrows indicate c-Jun or GATA-6+ cells. Data are presented as mean±SEM. Data were analyzed by 2-way ANOVA test followed by the Tukey multiple comparisons test (**A**–**F**). CAS indicates castration; CD, cluster of differentiation; DMSO, dimethyl sulfoxide; p-c-Jun, phosphorylated c-Jun; p-GSK-3β, phosphorylated GSK-3β; and T, testosterone.

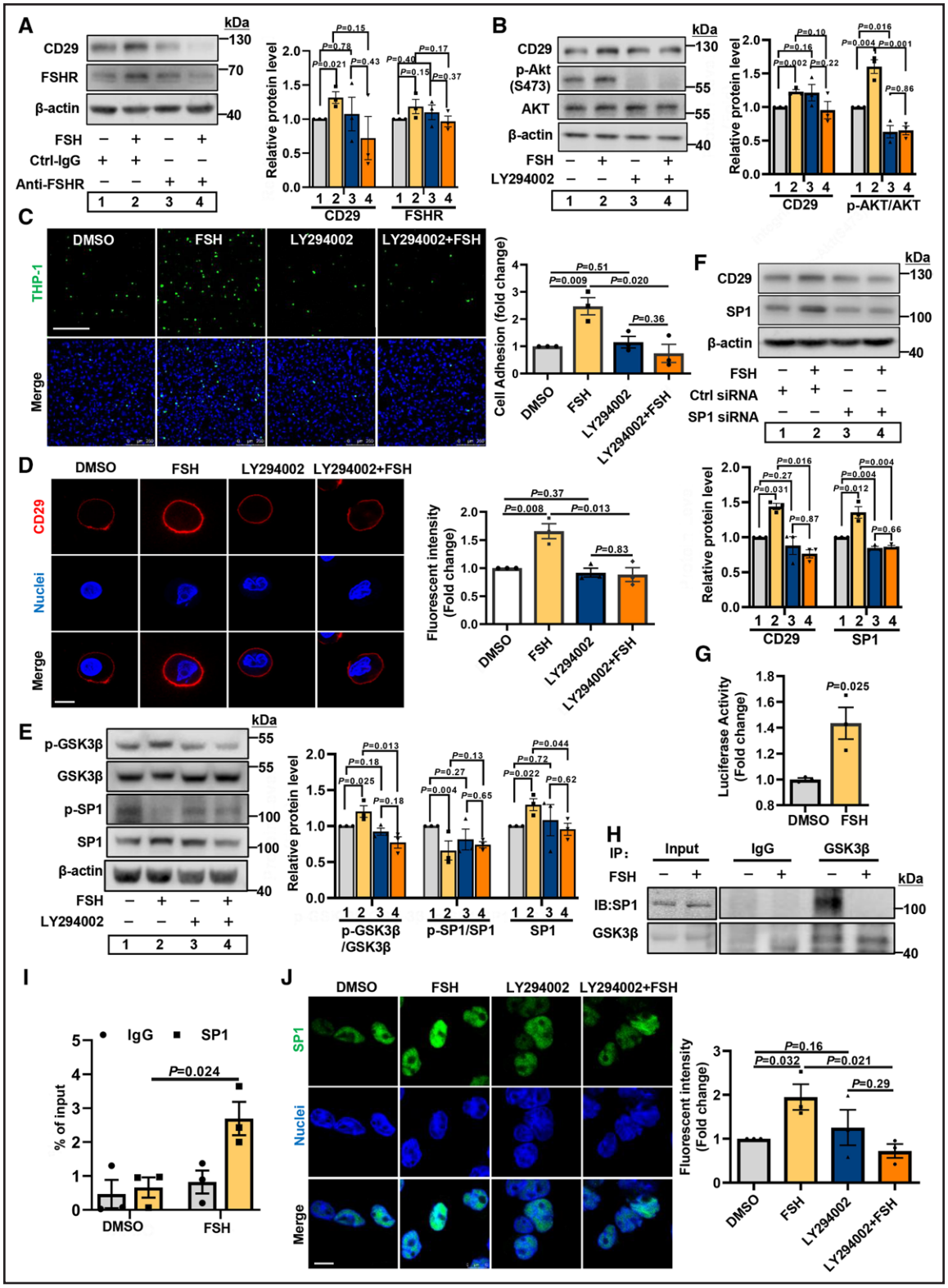

Figure 7. Follicle-stimulating hormone (FSH) upregulated CD29 (cluster of differentiation 29) expression through the PI3K (phosphatidylinositol 3 kinase)/AKT (protein kinase B)/GSK-3β (glycogen synthase kinase 3 beta)/SP1 (specificity protein 1) signal transduction pathway.

A through **E** and **J**, Human monocytic THP-1 cells were pretreated with anti-FSHR (FSH receptor) antibody for 1 hour or with the PI3K inhibitor LY294002 (10 μM) for 3 hours and then treated with FSH (50 ng/mL) for 24 hours. **F** and **J**, THP-1 cells were transfected with SP1 siRNAs for 24 hours and then treated with or without FSH. **A**, Effects of FSHR blockade on CD29 expression in THP-1 cells with the indicated treatment. β-actin served as a loading control (Ctrl); n=3 biological replicates. **B**, Effects of PI3K inhibition on the expression of CD29 in THP-1 cells. Phosphorylated AKT (p-AKT) and total AKT were also detected to indicate the effectiveness of inhibitors; (*Continued*)

Intraluminal Inhibition of FSHR Ameliorates Endothelial Inflammation and Atherosclerosis

Our data suggest that FSHR may be an accessible therapeutic target to prevent atherosclerosis. To test its feasibility, we intraluminally applied specific FSHR shRNA adenovirus in common carotid arteries of *ApoE*$^{-/-}$ mice that were then subjected to partial carotid artery ligation and Leu administration for 4 weeks (Figure 8A). Immunofluorescence staining clearly showed that FSHR expression in the carotid artery was significantly knocked down by adenovirus vector with FSHR-targeted shRNA as compared with the control group (Figure S12). Analysis results revealed that, compared with saline, Leu administration caused dramatic intima thickening (Figure 8B and 8C) and plaque growth (Figure 8D and 8E) in the ligated carotid arteries, where blood flow was disturbed. Most importantly, Leu-induced intima thickening and plaque growth were markedly attenuated by intraluminal adenovirus vector with FSHR-targeted shRNA pretreatment (Figure 8C and 8E). Furthermore, as shown by immunostaining, adenovirus vector with FSHR-targeted shRNA remarkably ameliorated Leu-induced VCAM-1 (Figure 8F) and GATA-6 (Figure 8G) expression in the atherosclerotic lesion of carotid arteries. The data strongly demonstrated the beneficial effect of endothelial FSHR blocking in preventing GnRH agonist–induced atherosclerosis.

DISCUSSION

Till now, the mechanisms for ADT-associated CVDs remain unclear. Multiple lines of evidence showing that the risk of cardiac events is significantly lower among men treated with GnRH antagonist compared with GnRH agonist suggest that testosterone deficiency is not the only reason for CVD development, and other factors may be involved.[25,34,52–54] Here, we demonstrated that FSH, either persistently or transiently elevated by orchiectomy or GnRH agonist, plays an essential role in accelerating the development of atherosclerosis by exaggerating endothelial inflammation and promoting monocyte-endothelial adhesion, thus providing a mechanism for ADT-associated CVDs (Figure 8H).

In addition to traditional ADTs studied in this work, CYP17A1 (cytochrome P450 17A1) inhibitors (eg, abiraterone) are used to suppress androgen production from the adrenal gland to treat patients with metastatic castration resistant PCa and grouped under the umbrella of ADTs in many studies.[55] A recent meta-analysis revealed that abiraterone stood out for increasing risk of cardiac events among all ADTs.[5] Since abiraterone also inhibits androgen production from testis, its administration would result in the lowest androgen level[56] and in turn the highest FSH level among ADTs. Whether high FSH level contributes to abiraterone-associated high risk of cardiac events should be investigated in other species since mouse is lack of postnatal expression of *Cyp17a1*.[57]

The metabolic abnormalities, including dyslipidemia, insulin resistance, and increasing body weight, were considered one of the reasons for ADT-associated CVDs, which may be possibly caused by loss of androgen or GnRH agonist.[58–60] In our mouse models, Leu-administered or surgically castrated *ApoE*$^{-/-}$ mice had no difference with control mice in their serum TC, TG, HDL, and LDL levels or body weights. Lipidomics analysis further showed similar phospholipid profiles between Leu-administered and control mice (Figure 2H and 2I). These suggest that dyslipidemia is not the major reason for GnRH agonist–associated or orchiectomy-associated CVDs. Yet, Deg-administered mice were found to have increased HDL level, significant body weight loss, and importantly, a distinct phospholipid profile as compared with control or Leu-administered mice. It has been shown that inhibiting ceramide biosynthesis in mice and rats prevents the development of hypertension, atherosclerosis, diabetes, and heart failure.[61] The reduction of ceramides in Deg-treated mice might have a protective effect on atherosclerosis. Meanwhile, because the FSH level continuously remains low after GnRH antagonist treatment, the proatherogenic effect of FSH as revealed in the present study would be avoided. Therefore, the beneficial alterations in lipid metabolism and the low FSH level should be 2 major reasons for the low CVD risk in GnRH antagonist administration. Our finding that GnRH antagonist had lower CVD risk than other ADTs is consistent with animal studies conducted in both *ApoE*$^{-/-}$[62]

Figure 7 Continued. n=3 biological replicates. **C**, The effects of PI3K inhibition on THP-1 cell adhesion to human umbilical vein endothelial cells (HUVECs). Scale bar, 300 μm. Data were from images of 3 biological replicates. **D**, Effects of PI3K inhibition on membrane CD29 distribution in THP-1 cells. Data were from images of 3 biological replicates. **E**, The effects of PI3K inhibition on the expression of phosphorylated GSK-3β (p-GSK-3β), total GSK-3β, phosphorylated SP1 (p-SP1), and total SP1 in THP-1 cells; n=3 biological replicates. **F**, Effects of SP1 knockdown on the expression of CD29 in THP-1 cells. β-actin served as a loading Ctrl; n=3 biological replicates. **G**, Effects of FSH on SP1 transcriptional activity. THP-1 cells were transfected with a specific dual-luciferase system that contains multiple SP1-binding sites. After 24 hours of transfection, THP-1 cells were exposed to FSH for 24 hours. The relative luciferase represents SP1 transcriptional activity; n=3 biological replicates. **H**, The effects of FSH on the association of GSK-3β and SP1 in THP-1 cells. GSK-3β antibody was used to coimmunoprecipitate SP1 with or without FSH treatment in THP-1 cells. **I**, Enrichment of SP1 on the CD29 promoter as determined by the chromatin immunoprecipitation assay in THP-1 cells with indicated treatment for 6 hours. IgG was served as negative Ctrl; n=3 biological replicates. **J**, Effects of FSH on SP1 cellular location. Immunofluorescence staining showed SP1 localization in THP-1 cells treated with FSH for 12 hours. Scale bar, 10 μm. Data were from images of 3 biological replicates. Data are presented as mean±SEM. Data were analyzed by 2-way ANOVA test followed by the Tukey multiple comparisons test (**A**, **B**, **E**, **F**, and **I**) and by 1-way ANOVA test followed by the Tukey multiple comparisons test (**C** and **D**). Data in **G** were analyzed by unpaired, 2-tailed Student *t* test. IB indicates immunoblotting; and IP, immunoprecipitation.

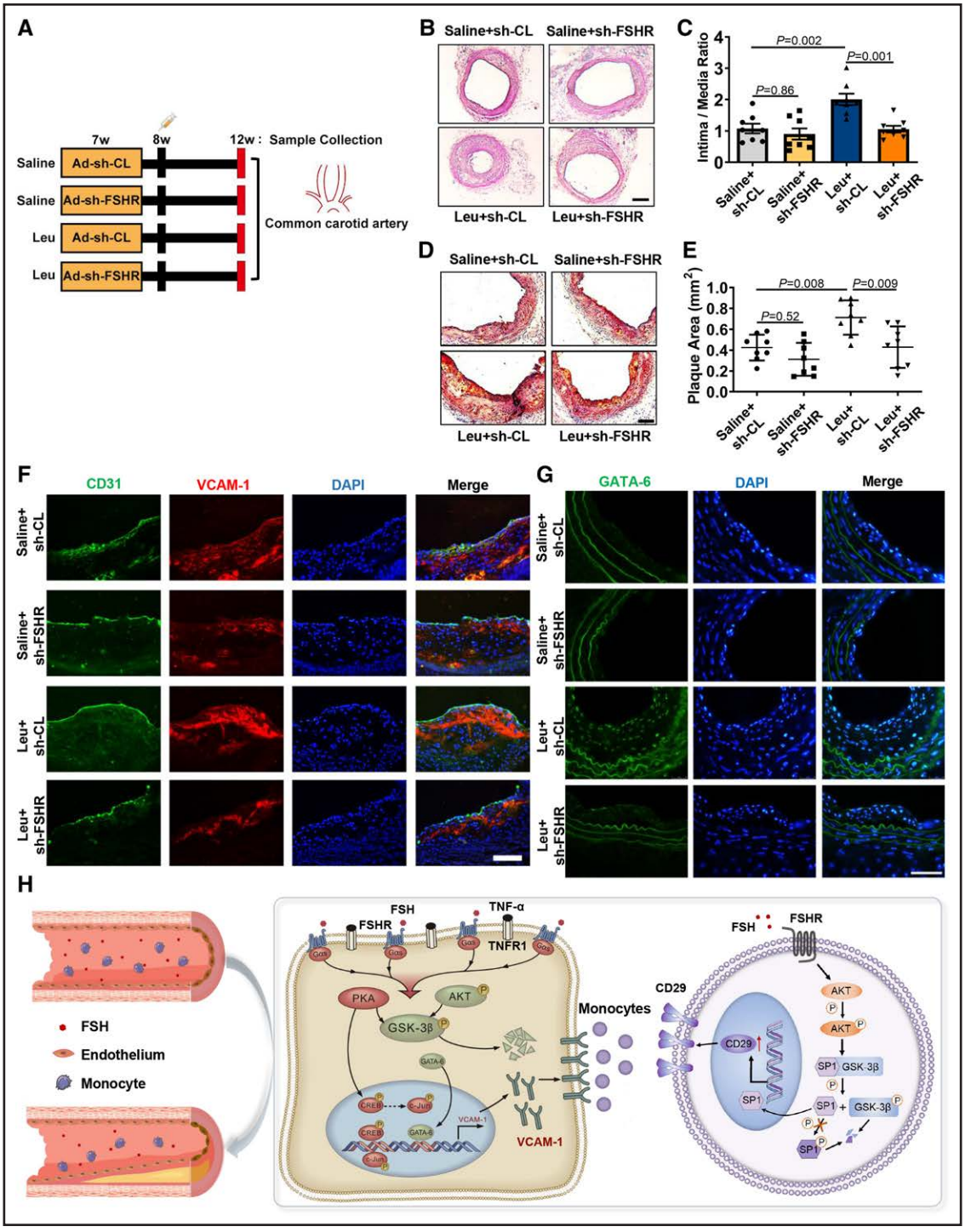

Figure 8. Intraluminal inhibition of FSHR (follicle-stimulating hormone receptor) ameliorated endothelial inflammation and atherosclerosis.

A, The experimental design in which *ApoE*$^{-/-}$ mice were subjected to partial carotid ligation incubated with adenovirus vector with FSHR-targeted shRNA (Ad-sh-FSHR) or control virus at 7 weeks and then subcutaneously injected with saline or leuprolide (Leu) at 8 weeks. Mice were fed a Western diet and euthanized at 12 weeks. **B** and **C**, Representative images of hematoxylin & eosin (H&E)-stained ligated carotid arteries (**B**) and quantification of the intima/media ratio (**C**) of mice in the saline+Ad-sh-CL, saline+Ad-sh-FSHR, Leu+Ad-sh-CL, and Leu+Ad-sh-FSHR groups (n=8 mice). Scale bar, 100 μm. **D** and **E**, Representative images of oil red O–stained ligated carotid arteries (**D**) and quantification of plaques in the common carotid arteries of each group (**E**); n=8 mice. **F**, Representative images of VCAM-1 (vascular cell adhesion protein 1; red) expression in the endothelium (CD31 [cluster of differentiation 31] positive, red) from the common carotid arteries of 12-week-old mice (n=8) were determined using immunofluorence (IF). Scale bar, 100 μm. **G**, Representative images of GATA-6 (GATA-binding protein 6; green) expression colocalized with DAPI (4′,6-diamidino-2-phenylindole) from the common carotid arteries using IF. Scale bar, 50 μm. **H**, Proposed mechanisms of follicle-stimulating hormone (FSH) in atherosclerosis progression. Data are presented as mean±SEM. (*Continued*)

and *LDLR*$^{-/-}$[23] mice. But there are also some researchers who found no difference between all 3 ADTs.[52,63] This discrepancy may be originated from the diversity in drug dosage, drug administration, and feeding diet used in these studies. In addition, one unexpected result was that Deg-administered mice had much higher liver TC and TG than control and Leu-administered mice (Figure S3G and S3H). This indicates that the effects of GnRH antagonist on lipid metabolism were rather complicated and need further investigation.

It has been reported that FSH induces dyslipidemia and fat accumulation in mouse and human.[30,38,64,65] Since FSH levels are high in castrated, castration+testosterone+FSH, and FSH-administered noncastrated mice, or transiently high in Leu-administered mice, one would expect that they may have more blood lipids and adipose lipids than their corresponding control mice. We found that adipose TC in castration+testosterone+FSH mice was significantly higher than that in castration+testosterone mice (Figure S1H), suggesting that FSH indeed induced lipid accumulation in fat, but no difference was found in adipose TC in other groups of mice (Figures S1 through S3). Furthermore, we did not observe significant change in blood lipids in all these groups. This phenomena could be explained by the variation of testosterone levels, transient change of the FSH level, or the lipid deposits in liver in these mice. This finding suggests that the effects of FSH on lipid metabolism and fat accumulation did not contribute to its proatherogenic function and ADT-associated CVDs.

It is thought that ADT with GnRH agonist likely has direct effects on cells of the cardiovascular system that express AR, GnRH receptor, or FSHR.[24,66] We found that supplement of Bica, a selective antagonist of AR, in Leu-administered mice showed a limited alleviating effect on plaque formation (Figure 2D and 2E) and reduced macrophage infiltration in the plaque (Figure 2F). It has been reported that global AR knockout (KO) accelerated atherogenesis in noncastrated male and female mice, suggesting AR-mediated inhibition of lesion formation.[67,68] But strikingly, macrophage-selective *ARKO/LDLR*$^{-/-}$ mice had reduced atherosclerotic lesion area and decreased infiltration of macrophages in plaques, implying a proatherogenic role for macrophage AR.[69] This may explain the positive effect of Bica in Leu-administered mice and indicates the involvement of macrophage AR in Leu-related CVDs. GnRH agonist itself had no influence on endothelial cell inflammation or monocyte adhesion (Figures S5A and S8G), suggesting that the GnRH receptor may not be directly involved in GnRH agonist–associated CVDs. FSHR is found expressed in endothelial cells and monocytes. Since FSH elevation occurs in ADT with GnRH agonist administration or surgical castration, it would be interesting to investigate the effects of FSH on both cell types.

Previous study has shown that FSH alone could promote VCAM-1 expression in HUVECs through the FSHR/Gαs (G-protein alpha s)/cAMP/PKA and the PI3K/AKT/mTOR (mammalian target of rapamycin)/NF-κB pathways.[27,29] But in our hands, FSH alone had no effect on the expression of VCAM-1 and other adhesion molecules in HUVECs. Rather, FSH, by synergizing with TNF-α, exaggerated endothelial inflammation (expression of adhesion molecules and MCP-1; Figure 4). This discrepancy may come from the differences in dose and duration of FSH treatment that we utilized. Since several clinical studies have shown that ADT increases cardiac events mainly in patients with preexisting CVDs,[21,70,71] who have increased level of proinflammatory factors, such as TNF-α, IL-6, and IL-1β,[72] our finding may provide a reasonable explanation for this phenomenon. Importantly, in addition to TNF-α, FSH also had a synergistic effect with IL-1β on promoting endothelial inflammation, which is also true in human aortic endothelial cells (Figure S7). This makes FSH a strong proinflammatory enhancer since it exaggerates the effects of multiple proinflammatory factors on endothelium. Although distinct mechanisms exist for the regulation of VCAM-1 by TNF-α,[73] we showed that cAMP/PKA/CREB/c-Jun and PI3K/AKT/GSK-3β/GATA-6 were 2 major pathways responsible for FSH+TNF-α–induced VCAM-1 upregulation in endothelial cells (Figure 6). It is interesting to notice that FSH alone could activate these pathways, but apparently, it was not strong enough to promote VCAM-1 expression, if not synergized with TNF-α. In addition, we found that both TNF-α and FSH could upregulate FSHR expression in endothelial cells (data not shown). There might exist a positive feedback loop augmenting the synergistic action of FSH and TNF-α. It should be pointed out that the advantageous effect of the PI3K/AKT pathway is often emphasized in ECs because it leads to the activation of eNOS (endothelial NO synthase).[74–76] But a large body of literature showed the adverse functions of PI3K/AKT in ECs, referring to endothelial injury, inflammation, permeability, barrier integrity, and so on.[50,73,77–80] We showed that the PI3K/AKT/GSK-3β/GATA-6 pathway together with the cAMP/PKA/CREB/c-Jun pathway participated in FSH+TNF-α–induced endothelial inflammation (Figure 6).

It has been found that FSH, binding to its receptor, could increase the expression of RANK (receptor activator of nuclear factor-kappa B) on peripheral blood monocytes.[81] Here, we showed that FSH upregulated CD29 on

Figure 8 Continued. Data were analyzed by 2-way ANOVA test followed by the Tukey multiple comparisons test (**C** and **E**). Ad-sh-CL indicates adenovirus vector with control-targeted shRNA; AKT, protein kinase B; CREB, cAMP response element-binding protein; Gαs, G-protein alpha s; GSK-3β, glycogen synthase kinase 3 beta; PKA, protein kinase A; SP1, specificity protein 1; TNF-α, tumor necrosis factor alpha; and TNFR1, tumor necrosis factor receptor 1.

human monocytes through the PI3K/AKT/GSK-3β/SP1 pathway and promoted monocyte adhesion to endothelial cells both in vitro and in vivo (Figures 5 and 7). In addition to CD29, another adhesion molecule, L-selectin, was also upregulated by FSH. Increased expression of adhesion molecules on monocytes and exacerbated VCAM-1 expression on endothelial cells would greatly promote monocyte-endothelial adhesion, which explains the accelerated lesion formation seen in Leu-administered or castrated mice. It is possible that monocyte adhesion driven, in part, by FSH may provide the inflammatory stimulus needed to induce endothelial inflammation, especially since FSH alone had no effect on ECs in vitro. Once infiltrating into the plaque, monocytes would be activated by RANKL (RANK ligand) released by Th1 (T-helper cell type I) cells and differentiated into osteoclasts, which could reabsorb calcified regions within the plaque and contribute to plaque instability.[82] This could be one of the reasons for the unstable plaques found in Leu-administered mice. In addition, monocytes differentiate into macrophages after they infiltrate into the vessel wall. We recently found that FSH promoted the expression of IL-1β in macrophages and accelerated their chemotactic migration, but the later effect was eliminated in the presence of oxidized LDL.[32] Although the underlying mechanisms need to be determined, these observations suggest that FSH may promote the accumulation of macrophages and induce local inflammation in the plaques, which would contribute to the growth of atherosclerotic lesion.

Different ADT modalities induce distinct patterns of FSH alterations. Surgical castration caused long-term high FSH level in mice. The daily supplement of testosterone or testosterone+FSH in castrated mice for 3 months gave rise to normal or long-term high FSH level, respectively. We observed extensive expressions and secretion of adhesion molecules in endothelium and serum in castrated and castration+testosterone+FSH mice but not in Sham and castration+testosterone mice (Figure 1; Figure S6), indicating a correlation between long-term high FSH and endothelial inflammation. It would be meaningful to collect blood from ADT patients at the indicated time point to validate associations between FSH and adhesion molecules before and after ADT. Notably, *ApoE*$^{-/-}$ mice show higher levels of serum TNF-α compared with wild-type mice and 12-week Western diet regimen induces systemic production of TNF-α,[83] thus our in vitro experimental condition well imitates the in vivo condition. Consistent with in vivo data, FSH+TNF-α synergistically exaggerated endothelial inflammation, suggesting that long-term FSH elevation in the context of orchiectomy accelerated atherosclerosis mainly by aggravating endothelial inflammation.

Compared with long-term elevation of FSH in the orchiectomy model, GnRH agonist induces FSH elevation for only 2 or 3 weeks followed by a gradual decrease. Although microsurges exists on repeat injection, the level of FSH remains far below the normal range.[22,23] Would transient FSH surge still contribute to the acceleration of atherogenesis in the context of GnRH agonist? This question was well answered by the experiments performed on Leu- or Deg-administered mice (Figures 2 and 3). In Leu-treated mice, anti-FSHβ antibody alleviated atherogenesis, and in Deg-treated mice, 2 weeks' addition of FSH significantly increased atherosclerosis. These data demonstrated the critical role of transient FSH surge in GnRH agonist–associated atherogenesis. One would expect that the orchiectomy model may develop larger lesions than the GnRH agonist model because of its long-term FSH elevation. However, we found that the lesion sizes were comparable in these 2 models (0.679±0.054 versus 0.646±0.039 mm^3; P=0.78) and this observation was consistent with previous reports.[23] This may exactly point out the importance of clinical flare of FSH in the acceleration of atherogenesis,

How can the short FSH surge associated with GnRH agonist treatment have such long-standing effects on atherosclerosis? One reason lies in the prolonged endothelial inflammation induced by short-term FSH treatment. In vitro, in the presence of TNF-α, mere 6-hour pretreatment of FSH led to prolonged VCAM-1 and E-selectin expression till 48 hours (Figure 4J and 4K), which may be due to the long activation period of FSHR downstream pathways. Another possible reason could be the upregulation of FSHR by both TNF-α and FSH (data not shown). Elevated FSHR expression on endothelial cells may increase their sensitivity to circulating FSH even when it is at a low concentration. Since endothelial inflammation and monocyte adhesion are the early events of atherosclerosis, the increased occurrence of these early events would make the effects of short-term FSH elevation persist for a long time. In addition, long-standing effects of the short FSH surge suggest that FSH may induce epigenetic changes in vascular cells and immune cells. This would be an interesting topic to study. Despite this, our data suggest that avoiding FSH fluctuation or blocking FSH/FSHR activity would be critical when ADT is applied. It is noticed that anti-FSHβ antibody did not completely eliminate the effect of FSH (Figure 3B and 3C). This suggests that dose or administration of FSHβ antibody needs to be optimized, or new strategies, such as FSH/FSHR inhibitors, should be developed.

To this end, a strategy of intraluminal administration of FSHR shRNA adenovirus was applied in a mouse model of atherosclerosis in which partial carotid ligation was combined with high-fat diet.[84] The data clearly demonstrated that specific inhibition of FSHR in endothelial cells significantly alleviated Leu-induced atherosclerosis (Figure 8). Furthermore, endothelial inflammation was also significantly hampered by FSHR shRNA. These findings validated the feasibility of blocking FSHR in preventing atherosclerosis. Importantly, they also identified the critical role of FSH-induced endothelial inflammation in GnRH agonist–associated atherosclerosis.

The lower CVD risk makes GnRH antagonist a good choice for patients with PCa. But till now, GnRH agonist is still the dominant type of ADT worldwide. In China, GnRH antagonist has been approved by the Center for Drug Evaluation but not been widely used so far. Our study suggests that strategies targeting FSH/FSHR or cardioprotective drugs should be considered to prevent the occurrence of CVDs in patients with PCa treated with GnRH agonist or orchiectomy.

ARTICLE INFORMATION

Received April 11, 2023; accepted December 21, 2023.

Affiliations

Department of Urology, Peking University People's Hospital, Beijing, China (Q.W., J.H., Y.D., T.X.). Department of Physiology and Pathophysiology, Hemorheology Center, School of Basic Medical Sciences, Peking University, Beijing, China (Z.L., X.G., J.Z., W.Y.). Key Laboratory of Molecular Cardiovascular Sciences, Ministry of Education, Beijing, China (Z.L., X.G., J.Z., W.Y.). Department of Urology, Sichuan Cancer Hospital, Sichuan Cancer Center, School of Medicine, University of Electronic Science and Technology of China, Chengdu (Q.W.). Department of Integration of Chinese and Western Medicine, School of Basic Medical Sciences, Peking University, Beijing, China (W.Y.).

Acknowledgments

The authors would like to thank Fang Yu and Jing Zhao at the Department of Physiology and Pathophysiology, School of Basic Medical Sciences, Peking University Health Science Center, for their help in flow cytometry and immunofluorescence staining. They thank Dr Xunde Xian at Institute of Cardiovascular Sciences, School of Basic Medical Sciences, Peking University Health Science Center, for his suggestions on the lipid analyses of our animal models. They also thank Wenting Li at the Department of Laboratory Animal Science, Peking University Health Science Center, for her useful instructions of animal experiments.

Sources of Funding

This work is funded by the National Natural Science Foundation of China (No. 82071777 to T. Xu; No. 32171143, 31570938, 31771280, and 11732001 to W. Yao; and No. 32325030 to J. Zhou), the Interdisciplinary Medicine Seed Fund of Peking University (BMU2017MX012 and BMU2020MX002 to T. Xu and BMU2018MX012 to T. Xu and W. Yao), and the China Urologic Cancer Research Foundation from Beijing Life Oasis Public Service Center (No. 2023-Z-16 to T. Xu).

Disclosures

None.

Supplemental Material

Supplemental Methods
Figures S1–S12
Table S1
Lipidomics Data Set
Videos S1–S3
Major Resources Table
Uncropped Gels

REFERENCES

1. Wong MCS, Goggins WB, Wang HHX, Fung FDH, Leung C, Wong SYS, Ng CF, Sung JJY. Global incidence and mortality for prostate cancer: analysis of temporal patterns and trends in 36 countries. *Eur Urol*. 2016;70:862–874. doi: 10.1016/j.eururo.2016.05.043
2. Siegel RL, Miller KD, Jemal A. Cancer statistics, 2020. *CA Cancer J Clin*. 2020;70:7–30. doi: 10.3322/caac.21590
3. Shi F, Xia S. Hormonal therapy and overall management of prostate cancer. *Chinese J Cancer Biother*. 2018;25:23–27. doi: 10.3872/j.issn.1007-385x.2018.01.004
4. Desai K, McManus JM, Sharifi N, Hormonal therapy for prostate cancer, *Endocrine Reviews*. 2021;42:354–373. doi: 10.1210/endrev/bnab002
5. Hu JR, Duncan MS, Morgans AK, Brown JD, Meijers WC, Freiberg MS, Salem J-E, Beckman JA, Moslehi JJ. Cardiovascular effects of androgen deprivation therapy in prostate cancer: contemporary meta-analyses. *Arterioscler Thromb Vasc Biol*. 2020;40:e55–e64. doi: 10.1161/ATVBAHA.119.313046
6. O'Farrell S, Garmo H, Holmberg L, Adolfsson J, Stattin P, Van Hemelrijck M. Risk and timing of cardiovascular disease after androgen-deprivation therapy in men with prostate cancer. *J Clin Oncol*. 2015;33:1243–1251. doi: 10.1200/JCO.2014.59.1792
7. Keating NL, O'Malley AJ, Smith MR. Diabetes and cardiovascular disease during androgen deprivation therapy for prostate cancer. *J Clin Oncol*. 2006;24:4448–4456. doi: 10.1200/JCO.2006.06.2497
8. Keating NL, O'Malley AJ, Freedland SJ, Smith MR. Diabetes and cardiovascular disease during androgen deprivation therapy: observational study of veterans with prostate cancer. *J Natl Cancer Inst*. 2010;102:39–46. doi: 10.1093/jnci/djp404
9. Bosco C, Bosnyak Z, Malmberg A, Adolfsson J, Keating NL, Van Hemelrijck M. Quantifying observational evidence for risk of fatal and nonfatal cardiovascular disease following androgen deprivation therapy for prostate cancer: a meta-analysis. *Eur Urol*. 2015;68:386–396. doi: 10.1016/j.eururo.2014.11.039
10. Bosco C, Crawley D, Adolfsson J, Rudman S, Van Hemelrijck M. Quantifying the evidence for the risk of metabolic syndrome and its components following androgen deprivation therapy for prostate cancer: a meta-analysis. *PLoS One*. 2015;10:e0117344–e0117312. doi: 10.1371/journal.pone.0117344
11. Meng F, Zhu S, Zhao J, Vados L, Wang L, Zhao Y, Zhao D, Niu Y. Stroke related to androgen deprivation therapy for prostate cancer: a meta-analysis and systematic review. *BMC Cancer*. 2016;16:180. doi: 10.1186/s12885-016-2221-5
12. Weiner AB, Li EV, Desai AS, Press DJ, Schaeffer EM. Cause of death during prostate cancer survivorship: a contemporary, US population-based analysis. *Cancer*. 2021;127:2895–2904. doi: 10.1002/cncr.33584
13. Ye Y, Zheng Y, Miao Q, Ruan H, Zhang X. Causes of death among prostate cancer patients aged 40 years and older in the United States. *Front Oncol*. 2022;12:914875. doi: 10.3389/fonc.2022.914875
14. Tietge UJF. Hyperlipidemia and cardiovascular disease: inflammation, dyslipidemia, and atherosclerosis. *Curr Opin Lipidol*. 2014;25:94–95. doi: 10.1097/MOL.0000000000000051
15. Gimbrone MA Jr, Guillermo GC. Endothelial cell dysfunction and the pathobiology of atherosclerosis. *Circ Res*. 2016;176:139–148. doi: 10.1161/CIRCRESAHA.115.306301
16. Kulkarni M, Bowman E, Gabriel J, Amburgy T, Mayne E, Zidar DA, Maierhofer C, Turner AN, Bazan JA, Koletar SL, et al. Altered monocyte and endothelial cell adhesion molecule expression is linked to vascular inflammation in human immunodeficiency virus infection. *Open Forum Infect Dis*. 2016;3:ofw224. doi: 10.1093/ofid/ofw224
17. Schnitzler JG, Dallinga-Thie GM, Kroon J. The role of (modified) lipoproteins in vascular function: a duet between monocytes and the endothelium. *Curr Med Chem*. 2019;26:1594–1609. doi: 10.2174/0929867325666180316121015
18. Tabas I, Bornfeldt KE. Macrophage phenotype and function in different stages of atherosclerosis. *Circ Res*. 2016;118:653–667. doi: 10.1161/CIRCRESAHA.115.306256
19. Ukkola O, Huttunen T, Puurunen VP, Piira OP, Niva J, Lepojärvi S, Tulppo M, Huikuri H. Total testosterone levels, metabolic parameters, cardiac remodeling and exercise capacity in coronary artery disease patients with different stages of glucose tolerance. *Ann Med*. 2013;45:206–212. doi: 10.3109/07853890.2012.711951
20. Jones TH, Kelly D. Randomized controlled trials - mechanistic studies of testosterone and the cardiovascular system. *Asian J Androl*. 2018;20:120. doi: 10.4103/aja.aja_6_18
21. Margel D, Peer A, Ber Y, Sela S, Shavit Grievink L, Tabachnik T, Witberg G, Baniel J, Kedar D, Duivenvoorden Wilhelmina CM, et al. Cardiovascular morbidity in a randomized trial comparing GnRH-agonist and antagonist among patients with advanced prostate cancer. *J Clin Oncol*. 2019;37:5015–5015. doi: 10.1200/jco.2019.37.15_suppl.5015
22. Klotz L, Boccon-Gibod L, Shore ND, Andreou C, Persson B-E, Cantor P, Jensen J-K, Olesen TK, Schröder FH. The efficacy and safety of degarelix: a 12-month, comparative, randomized, open-label, parallel-group phase III study in patients with prostate cancer. *BJU Int*. 2008;102:1531–1538. doi: 10.1111/j.1464-410X.2008.08183.x
23. Hopmans SN, Duivenvoorden WC, Werstuck GH, Klotz L, Pinthus JH. GnRH antagonist associates with less adiposity and reduced characteristics of metabolic syndrome and atherosclerosis compared with orchiectomy and GnRH agonist in a preclinical mouse model. *Urol Oncol*. 2014;32:1126–1134. doi: 10.1016/j.urolonc.2014.06.018

24. Poljak Z, Hulin I, Maruscakova L, Mladosievicova B. Are GnRH and FSH potentially damaging factors in the cardiovascular system? *Pharmazie*. 2018;73:187–190. doi: 10.1691/ph.2018.7992
25. Crawford ED, Tombal B, Keane T, Boccardo F, Miller K, Shore N, Moul JW, Damber JE, Collette L, Persson BE. FSH suppression and tumour control in patients with prostate cancer during androgen deprivation with a GnRH agonist or antagonist. *Scand J Urol*. 2018;52:349–357. doi: 10.1080/21681805.2018.1522372
26. Deiktakis EE, Ieronymaki E, Zarén P, Hagsund A, Wirestrand E, Malm J, Tsatsanis C, Huhtaniemi IT, Giwercman A, Giwercman YL. Impact of add-back FSH on human and mouse prostate following gonadotropin ablation by GnRH antagonist treatment. *Endocr Connect*. 2022;11:e210639. doi: 10.1530/EC-21-0639
27. Piao J, Yin Y, Zhao Y, Han Y, Zhan H, Luo D, Guo J. Follicle-stimulating hormone accelerates atherosclerosis by activating PI3K/Akt/NF-κB pathway in mice with androgen deprivation. *J Vasc Res*. 2022;59:358–368. doi: 10.1159/000527239
28. Munir JA, Wu H, Bauer K, Bindeman J, Byrd C, Feuerstein IM, Villines TC, Taylor AJ. The perimenopausal atherosclerosis transition: relationships between calcified and noncalcified coronary, aortic, and carotid atherosclerosis and risk factors and hormone levels. *Menopause*. 2012;19:10–15. doi: 10.1097/gme.0b013e318221bc8d
29. Li X, Chen W, Li P, Wei J, Cheng Y, Liu P, Yan Q, Xu X, Cui Y, Gu Z, et al. Follicular stimulating hormone accelerates atherogenesis by increasing endothelial VCAM-1 expression. *Theranostics*. 2017;7:4671–4688. doi: 10.7150/thno.21216
30. Liu XM, Chan HC, Ding GL, Cai J, Song Y, Wang TT, Zhang D, Chen H, Yu MK, Wu YT, et al. FSH regulates fat accumulation and redistribution in aging through the Gαi/Ca^{2+}/CREB pathway. *Aging Cell*. 2015;14:409–420. doi: 10.1111/acel.12331
31. Crawford ED, Schally AV. The role of FSH and LH in prostate cancer and cardiometabolic comorbidities. *Can J Urol*. 2020;27:10167–10173.
32. Han JL, Song YX, Yao WJ, Zhou J, Du Y, Xu T. Follicle-stimulating hormone provokes macrophages to secrete IL-1β contributing to atherosclerosis progression. *J Immunol*. 2023;210:25–32. doi: 10.4049/jimmunol.2200475
33. Margel D, Peer A, Ber Y, Shavit-Grievink L, Tabachnik T, Sela S, Witberg G, Baniel J, Kedar D, Duivenvoorden WCM, et al. Cardiovascular morbidity in a randomized trial comparing GnRH agonist and GnRH antagonist among patients with advanced prostate cancer and preexisting cardiovascular disease. *J Urol*. 2019;202:1199–1208. doi: 10.1097/JU.0000000000000384
34. Shore ND, Saad F, Cookson MS, George DJ, Saltzstein DR, Tutrone R, Akaza H, Bossi A, van Veenhuyzen DF, Selby B, et al; HERO Study Investigators. Oral relugolix for androgen-deprivation therapy in advanced prostate cancer. *N Engl J Med*. 2020;382:2187–2196. doi: 10.1056/NEJMoa2004325
35. Lopes RD, Higano CS, Slovin SF, Nelson AJ, Bigelow R, Sørensen PS, Melloni C, Goodman SG, Evans CP, Nilsson J, et al; PRONOUNCE Study Investigators. Cardiovascular safety of degarelix versus leuprolide in patients with prostate cancer: the primary results of the PRONOUNCE randomized trial [published correction appears in *Circulation*. 2021;144:e273]. *Circulation*. 2021;144:1295–1307. doi: 10.1161/CIRCULATIONAHA.121.056810
36. Daugherty A, Tall AR, Daemen MJAP, Falk E, Fisher EA, García-Cardeña G, Lusis AJ, Owens AP, Rosenfeld ME, Virmani R; American Heart Association Council on Arteriosclerosis, Thrombosis and Vascular Biology; and Council on Basic Cardiovascular Sciences. Recommendation on design, execution, and reporting of animal atherosclerosis studies: a scientific statement from the American Heart Association. *Arterioscler Thromb Vasc Biol*. 2017;37:e131–e157. doi: 10.1161/ATV.0000000000000062
37. Zhu LL, Blair H, Cao J, Yuen T, Latif R, Guo L, Tourkova IL, Li J, Davies TF, Sun L, et al. Blocking antibody to the β-subunit of FSH prevents bone loss by inhibiting bone resorption and stimulating bone synthesis. *Proc Natl Acad Sci USA*. 2012;109:14574–14579. doi: 10.1073/pnas.1212806109
38. Liu P, Ji Y, Yuen T, Rendina-Ruedy E, DeMambro VE, Dhawan S, Abu-Amer W, Izadmehr S, Zhou B, Shin AC, et al. Blocking FSH induces thermogenic adipose tissue and reduces body fat. *Nature*. 2017;546:107–112. doi: 10.1038/nature22342
39. Ivetic A, Hoskins Green HL, Hart SJ. L-selectin: a major regulator of leukocyte adhesion, migration and signaling. *Front Immunol*. 2019;10:1068. doi: 10.3389/fimmu.2019.01068
40. Kawakami A, Aikawa M, Alcaide P, Luscinskas FW, Libby P, Sacks FM. Apolipoprotein CIII induces expression of vascular cell adhesion molecule-1 in vascular endothelial cells and increases adhesion of monocytic cells. *Circulation*. 2006;114:681–687. doi: 10.1161/CIRCULATIONAHA.106.622514
41. Stilley JA, Guan R, Duffy DM, Segaloff DL. Signaling through FSH receptors on human umbilical vein endothelial cells promotes angiogenesis. *J Clin Endocrinol Metab*. 2014;99:E813–E820. doi: 10.1210/jc.2013-3186
42. Tu C, Fiandalo MV, Pop E, Stocking JJ, Azabdaftari G, Li J, Wei H, Ma D, Qu J, Mohler JL, et al. Proteomic analysis of charcoal-stripped fetal bovine serum reveals changes in the insulin-like growth factor signaling pathway. *J Proteome Res*. 2018;17:2963–2977. doi: 10.1021/acs.jproteome.8b00135
43. McCrohon JA, Jessup W, Handelsman DJ, Celermajer DS. Androgen exposure increases human monocyte adhesion to vascular endothelium and endothelial cell expression of vascular cell adhesion molecule-1. *Circulation*. 1999;99:2317–2322. doi: 10.1161/01.cir.99.17.2317
44. Gloaguen P, Crépieux P, Heitzler D, Poupon A, Reiter E. Mapping the follicle-stimulating hormone-induced signaling networks. *Front Endocrinol (Lausanne)*. 2011;2:45. doi: 10.3389/fendo.2011.00045
45. Ulloa-Aguirre A, Zariñán T, Jardón-Valadez E, Gutiérrez-Sagal R, Dias JA. Structure-function relationships of the follicle-stimulating hormone receptor. *Front Endocrinol (Lausanne)*. 2018;9:707. doi: 10.3389/fendo.2018.00707
46. Van Dam H, Castellazzi M. Distinct roles of Jun: Fos and Jun: ATF dimers in oncogenesis. *Oncogene*. 2001;20:2453–2464. doi: 10.1038/sj.onc.1204239
47. Casals-Casas C, Álvarez E, Serra M, de la Torre C, Farrera C, Sánchez-Tilló E, Caelles C, Lloberas J, Celada A. CREB and AP-1 activation regulates MKP-1 induction by LPS or M-CSF and their kinetics correlate with macrophage activation versus proliferation. *Eur J Immunol*. 2009;39:1902–1913. doi: 10.1002/eji.200839037
48. Iademarco MF, McQuillan JJ, Rosen GD, Dean DC. Characterization of the promoter for vascular cell adhesion molecule-1 (VCAM-1). *J Biol Chem*. 1992;267:16323–16329.
49. Glover CPJ, Heywood DJ, Bienemann AS, Deuschle U, Kew JNC, Uney JB. Adenoviral expression of CREB protects neurons from apoptotic and excitotoxic stress. *Neuroreport*. 2004;15:1171–1175. doi: 10.1097/00001756-200405190-00018
50. Tsoyi K, Jang HJ, Nizamutdinova IT, Park K, Kim YM, Kim HJ, Seo HG, Lee JH, Chang KC. PTEN differentially regulates expressions of ICAM-1 and VCAM-1 through PI3K/Akt/GSK-3β/GATA-6 signaling pathways in TNF-α-activated human endothelial cells. *Atherosclerosis*. 2010;213:115–121. doi: 10.1016/j.atherosclerosis.2010.07.061
51. Chen XH, Lu LL, Ke HP, Liu ZC, Wang HF, Wei W, Qi YF, Wang HS, Cai SH, Du J. The TGF-β-induced up-regulation of NKG2DLs requires AKT/GSK-3β-mediated stabilization of SP1. *J Cell Mol Med*. 2017;21:860–870. doi: 10.1111/jcmm.13025
52. Poulsen CB, Mortensen MB, Koechling W, Sørensen CB, Bentzon JF. Differences in hypercholesterolemia and atherogenesis induced by common androgen deprivation therapies in male mice. *J Am Heart Assoc*. 2016;5:e002800. doi: 10.1161/JAHA.115.002800
53. Wang FY, Tang XM, Wang X, Huang KB, Feng HW, Chen ZF, Liu YN, Liang H. Mitochondria-targeted platinum(II) complexes induce apoptosis-dependent autophagic cell death mediated by ER-stress in A549 cancer cells. *Eur J Med Chem*. 2018;155:639–650. doi: 10.1016/j.ejmech.2018.06.018
54. Chen DY, Su PJ, See LC, Liu JR, Chuang CK, Pang ST, Tseng CN, Chen SW, Hsieh IC, Chu PH, et al. Gonadotropin-releasing hormone antagonist associated with lower cardiovascular risk compared with gonadotropin-releasing hormone agonist in prostate cancer: a nationwide cohort and in vitro study. *Prostate*. 2021;81:902–912. doi: 10.1002/pros.24187
55. Potter GA, Barrie SE, Jarman M, Rowlands MG. Novel steroidal inhibitors of human cytochrome P45017 alpha (17 alpha-hydroxylase-C17,20-lyase): potential agents for the treatment of prostatic cancer. *J Med Chem*. 1995;38:2463–2471. doi: 10.1021/jm00013a022
56. de Bono JS, Logothetis CJ, Molina A, Fizazi K, North S, Chu L, Chi KN, Jones RJ, Goodman OB, Saad F, et al; COU-AA-301 Investigators. Abiraterone and increased survival in metastatic prostate cancer. *N Engl J Med*. 2011;364:1995–2005. doi: 10.1056/NEJMoa1014618
57. Dumontet T, Martinez A. Adrenal androgens, adrenarche, and zona reticularis: a human affair? *Mol Cell Endocrinol*. 2021;528:111239. doi: 10.1016/j.mce.2021.111239
58. Navarro G, Allard C, Xu W, Mauvais-Jarvis F. The role of androgens in metabolism, obesity and diabetes in males and females. *Obesity (Silver Spring)*. 2015;23:713–719. doi: 10.1002/oby.21033
59. Hu X, Rui L, Zhu T, Xia H, Yang X, Wang X, Liu H, Lu Z, Jiang H. Low testosterone level in middle-aged male patients with coronary artery disease. *Eur J Intern Med*. 2011;22:e133–e136. doi: 10.1016/j.ejim.2011.08.016
60. Kintzel PE, Chase SL, Schultz LM, O'Rourke TJ. Increased risk of metabolic syndrome, diabetes mellitus, and cardiovascular disease in men receiving androgen deprivation therapy for prostate cancer. *Pharmacotherapy*. 2008;28:1511–1522. doi: 10.1592/phco.28.12.1511
61. Choi RH, Tatum SM, Symons JD, Summers SA, Holland WL. Ceramides and other sphingolipids as drivers of cardiovascular disease. *Nat Rev Cardiol*. 2021;18:701–711. doi: 10.1038/s41569-021-00536-1

62. Von Dehn G, Von Dehn O, Völker W, Langer C, Weinbauer GF, Behre HM, Nieschlag E, Assmann G, von Eckardstein A. Atherosclerosis in apolipoprotein E-deficient mice is decreased by the suppression of endogenous sex hormones. *Horm Metab Res*. 2001;33:110–114. doi: 10.1055/s-2001-12405
63. Duivenvoorden WCM, Naeim M, Hopmans SN, Yousef S, Werstuck GH, Dason S, Pinthus JH. Protective effect of pharmacological castration on metabolic perturbations and cardiovascular disease in the hyperglycemic male ApoE-/-:Ins2+/Akita mouse model. *Prostate Cancer Prostatic Dis*. 2021;24:389–397. doi: 10.1038/s41391-020-00288-y
64. Guo Y, Zhao M, Bo T, Ma S, Yuan Z, Chen W, He Z, Hou X, Liu J, Zhang Z, et al. Blocking FSH inhibits hepatic cholesterol biosynthesis and reduces serum cholesterol. *Cell Res*. 2019;29:151–166. doi: 10.1038/s41422-018-0123-6
65. Song Y, Wang ES, Xing LL, Shi S, Qu F, Zhang D, Li J-Y, Shu J, Meng Y, Sheng J-Z, et al. Follicle-stimulating hormone induces postmenopausal dyslipidemia through inhibiting hepatic cholesterol metabolism. *J Clin Endocrinol Metab*. 2016;101:254–263. doi: 10.1210/jc.2015-2724
66. Tivesten Å, Pinthus JH, Clarke N, Duivenvoorden W, Nilsson J. Cardiovascular risk with androgen deprivation therapy for prostate cancer: potential mechanisms. *Urol Oncol Semin Orig Investig*. 2015;33:464–475. doi: 10.1016/j.urolonc.2015.05.030
67. Fagman JB, Wilhelmson AS, Motta BM, Pirazzi C, Alexanderson C, De Gendt K, Verhoeven G, Holmäng A, Anesten F, Jansson JO, et al. The androgen receptor confers protection against diet-induced atherosclerosis, obesity, and dyslipidemia in female mice. *FASEB J*. 2015;29:1540–1550. doi: 10.1096/fj.14-259234
68. Bourghardt J, Wilhelmson AS, Alexanderson C, De Gendt K, Verhoeven G, Krettek A, Ohlsson C, Tivesten A. Androgen receptor-dependent and independent atheroprotection by testosterone in male mice. *Endocrinology*. 2010;151:5428–5437. doi: 10.1210/en.2010-0663
69. Huang CK, Pang H, Wang L, Niu Y, Luo J, Chang E, Sparks JD, Lee SO, Chang C. New therapy via targeting androgen receptor in monocytes/macrophages to battle atherosclerosis. *Hypertension*. 2014;63:1345–1353. doi: 10.1161/HYPERTENSIONAHA.113.02804
70. Hayes JH, Chen MH, Moran BJ, Braccioforte MH, Dosoretz DE, Salenius S, Katin MJ, Ross R, Choueiri TK, D'Amico AV. Androgen-suppression therapy for prostate cancer and the risk of death in men with a history of myocardial infarction or stroke. *BJU Int*. 2010;106:979–985. doi: 10.1111/j.1464-410X.2010.09273.x
71. Davey P, Kirby MG. Cardiovascular risk profiles of GnRH agonists and antagonists: real world analysis from UK general practice. *World J Urol*. 2021;39:307–315. doi: 10.1007/s00345-020-03433-3
72. Bruunsgaard H, Skinhøj P, Pedersen AN, Schroll M, Pedersen BK. Ageing, tumour necrosis factor-alpha (TNF-alpha) and atherosclerosis. *Clin Exp Immunol*. 2000;121:255–260. doi: 10.1046/j.1365-2249.2000.01281.x
73. Liu Y, Tie L. Apolipoprotein M and sphingosine-1-phosphate complex alleviates TNF-α-induced endothelial cell injury and inflammation through PI3K/AKT signaling pathway. *BMC Cardiovasc Disord*. 2019;19:279. doi: 10.1186/s12872-019-1263-4
74. Uruno A, Sugawara A, Kanatsuka H, Kagechika H, Saito A, Sato K, Kudo M, Takeuchi K, Ito S. Upregulation of nitric oxide production in vascular endothelial cells by all-trans retinoic acid through the phosphoinositide 3-kinase/Akt pathway. *Circulation*. 2005;112:727–736. doi: 10.1161/CIRCULATIONAHA.104.500959
75. Rizzo NO, Maloney E, Pham M, Luttrell I, Wessells H, Tateya S, Daum G, Handa P, Schwartz MW, Kim F. Reduced NO-cGMP signaling contributes to vascular inflammation and insulin resistance induced by high-fat feeding. *Arterioscler Thromb Vasc Biol*. 2010;30:758–765. doi: 10.1161/ATVBAHA.109.199893
76. Zhou J, Li YS, Chien S. Shear stress-initiated signaling and its regulation of endothelial function. *Arterioscler Thromb Vasc Biol*. 2014;34:2191–2198. doi: 10.1161/ATVBAHA.114.303422
77. Luo D, Zhao J, Rong J. Plant-derived triterpene celastrol ameliorates oxygen glucose deprivation-induced disruption of endothelial barrier assembly via inducing tight junction proteins. *Phytomedicine*. 2016;23:1621–1628. doi: 10.1016/j.phymed.2016.10.006
78. Bian C, Wu Y, Chen P. Telmisartan increases the permeability of endothelial cells through zonula occludens-1. *Biol Pharm Bull*. 2009;32:416–420. doi: 10.1248/bpb.32.416
79. Zhou Z, Gengaro P, Wang W, Wang X-qing, Li C, Faubel S, Rivard C, Schrier RW. Role of NF-kappaB and PI 3-kinase/Akt in TNF-alpha-induced cytotoxicity in microvascular endothelial cells. *Am J Physiol Renal Physiol*. 2008;295:F932–F941. doi: 10.1152/ajprenal.00066.2008
80. Murao K, Ohyama T, Imachi H, Ishida T, Cao WM, Namihira H, Sato M, Wong NC, Takahara J. TNF-α stimulation of MCP-1 expression is mediated by the Akt/PKB signal transduction pathway in vascular endothelial cells. *Biochem Biophys Res Commun*. 2000;276:791–796. doi: 10.1006/bbrc.2000.3497
81. Cannon JG, Kraj B, Sloan G. Follicle-stimulating hormone promotes RANK expression on human monocytes. *Cytokine*. 2011;53:141–144. doi: 10.1016/j.cyto.2010.11.011
82. Crawford ED, Schally AV, Pinthus JH, Block NL, Rick FG, Garnick MB, Eckel RH, Keane TE, Shore ND, Dahdal DN, et al. The potential role of follicle-stimulating hormone in the cardiovascular, metabolic, skeletal, and cognitive effects associated with androgen deprivation therapy. *Urol Oncol*. 2017;35:183–191. doi: 10.1016/j.urolonc.2017.01.025
83. Chen L, Liu W, Li Y, Luo S, Liu Q, Zhong Y, Jian Z, Bao M. Lactobacillus acidophilus ATCC 4356 attenuates the atherosclerotic progression through modulation of oxidative stress and inflammatory process. *Int Immunopharmacol*. 2013;17:108–115. doi: 10.1016/j.intimp.2013.05.018
84. Nam D, Ni CW, Rezvan A, Suo J, Budzyn K, Llanos A, Harrison D, Giddens D, Jo H. Partial carotid ligation is a model of acutely induced disturbed flow, leading to rapid endothelial dysfunction and atherosclerosis. *Am J Physiol Heart Circ Physiol*. 2009;297:H1535–H1543. doi: 10.1152/ajpheart.00510.2009